frontiers | Frontiers in Environmental Science

TYPE Review
PUBLISHED 14 November 2022
DOI 10.3389/fenvs.2022.1035865

OPEN ACCESS

EDITED BY
Huiyu Dong,
Chinese Academy of Sciences (CAS), China

REVIEWED BY
Zhihua Xiao,
Hunan Agricultural University, China
Yanling Gu,
Changsha University of Science and Technology, China

*CORRESPONDENCE
Zeeshan Ahmed,
zeeshanagronomist@yahoo.com
Rashid Iqbal,
rashid.iqbal@iub.edu.pk
Dong-Qin Dai,
cicidaidongqin@gmail.com

SPECIALTY SECTION
This article was submitted to Water and Wastewater Management, a section of the journal Frontiers in Environmental Science

RECEIVED 03 September 2022
ACCEPTED 14 October 2022
PUBLISHED 14 November 2022

CITATION
Murtaza G, Ahmed Z, Dai D-Q, Iqbal R, Bawazeer S, Usman M, Rizwan M, Iqbal J, Akram MI, Althubiani AS, Tariq A and Ali I (2022), A review of mechanism and adsorption capacities of biochar-based engineered composites for removing aquatic pollutants from contaminated water.
Front. Environ. Sci. 10:1035865.
doi: 10.3389/fenvs.2022.1035865

A review of mechanism and adsorption capacities of biochar-based engineered composites for removing aquatic pollutants from contaminated water

Ghulam Murtaza[1,2], Zeeshan Ahmed[3,4]*, Dong-Qin Dai[1]*, Rashid Iqbal[5]*, Sami Bawazeer[6], Muhammad Usman[7], Muhammad Rizwan[8], Javed Iqbal[9], Muhammad Irfan Akram[10], Abdullah Safar Althubiani[11], Akash Tariq[3,4] and Iftikhar Ali[12,13]

[1]Center for Yunnan Plateau Biological Resources Protection and Utilization, Yunnan Engineering Research Center of Fruit Wine, College of Biological Resource and Food Engineering, Qujing Normal University, Qujing, Yunnan, China, [2]Faculty of Environmental Science and Engineering, Kunming University of Science and Technology, Kunming, China, [3]Xinjiang Institute of Ecology and Geography, Chinese Academy of Sciences, Urumqi, Xinjiang, China, [4]Cele National Station of Observation and Research for Desert-Grassland Ecosystems, Chinese Academy of Sciences, Urumqi, Xinjiang, China, [5]Department of Agronomy, Faculty of Agriculture and Environment, The Islamia University of Bahawalpur, Bahawalpur, Punjab, Pakistan, [6]Department of Pharmacognosy, Umm Al- Qura University, Faculty of Pharmacy, Makkah, Saudi Arabia, [7]Department of Botany, Government College University, Lahore, Punjab, Pakistan, [8]School of Energy Science and Engineering, Central South University, Changsha, Hunan, China, [9]Department of Botany, Bacha Khan University, Charsadda, Khyber Pakhtunkhwa, Pakistan, [10]Department of Entomology, Faculty of Agriculture and Environment, The Islamia University of Bahawalpur, Bahawalpur, Punjab, Pakistan, [11]Department of Biology, Faculty of Applied Science, Umm Al-Qura University, Makkah, Saudi Arabia, [12]Center for Plant Sciences and Biodiversity, University of Swat, Charbagh, Khyber Pakhtunkhwa, Pakistan, [13]State Key Laboratory of Molecular Developmental Biology, Institute of Genetics and Developmental Biology, Chinese Academy of Sciences, Beijing, China

Water contamination by aquatic pollutants (antibiotics, heavy metals, nutrients, and organic pollutants) has become the most serious issue of recent times due to associated human health risks. Biochar (BC) has been deemed an effective and promising green material for the remediation of a wide range of environmental pollutants. Due to its limited properties (small pore size and low surface functionality), pristine BC has encountered bottlenecks in decontamination applications. These limitations can be rectified by modifying the pristine BC into engineered BC *via* multiple modification methods (physical, chemical, and mechanical), thus improving its decontamination functionalities. Recently, these engineered BCs/BC-based composites or BC composites have gathered pronounced attention for water decontamination due to fewer chemical requirements, high energy efficiency, and pollutant removal capacity. BC-based composites are synthesized by mixing BC with various modifiers, including carbonaceous material, clay minerals, metals, and metal oxides. They considerably modify the physiochemical attributes of BC and increase its adsorption ability against various types of aquatic pollutants. BC-based composites are efficient in

eliminating target pollutants. The efficiency and type of a specific mechanism depend on various factors, mainly on the physicochemical characteristics and composition of the BC-based composites and the target pollutants. Among the different engineered BCs, the efficiency of clay-BC composites in removing the antibiotics, dyes, metals, and nutrients was good. This review could help develop a comprehensive understanding of using engineered BCs as effective materials for the remediation of contaminated water. Finally, gaps and challenges in research are identified, and future research needs are proposed.

KEYWORDS

antibiotics, biochar, heavy metal, decontamination, sorption capacity

Introduction

Water contamination caused by antibiotics (Wu et al., 2022), nutrients, organic contaminants, and heavy metals is considered one of the most critical issues of recent times because of its alarming health risks to the ecological community, which needs sustainable and effective remediation approaches (Shaheen et al., 2022). Water decontamination methods using carbonaceous materials, including graphene, carbon nanotubes (CNT), activated carbon, and biochar (BC), have been developed to remove the impurities' detrimental effects on the water system (Hu et al., 2019). Among them, BC is the most effective and sustainable agent for water decontamination because of its diverse properties. BC is a carbon-enriched solid produced *via* pyrolyzing biomass without oxygen (Zhang et al., 2017). Usually, BC is prepared from various feedstocks such as solid wastes, animal litter, wood biomass, and agricultural residues by various thermochemical methods, including gasification, torrefaction, flash, and hydrothermal carbonization, fast pyrolysis, and slow pyrolysis (Tan et al., 2016a) (Table 1). The pristine BC has shown superior performance in water decontamination, but applications of pristine BC in decontamination have encountered bottlenecks because of its limited characteristics, which cannot meet the desired water remediation requirements. The engineering of BCs with various agents to improve their physicochemical attributes and sorption ability for better decontamination of water systems has emerged as a new trend (Wang et al., 2021).

The term "biochar-based engineered composite" is therefore used to denote engineered agents that have been loaded (metal oxides, CNT, clay minerals, and graphene) on BCs for specific purposes (Ok et al., 2015). Such composites can be synthesized *via* soaking BC with CNT, polysaccharides, carbonaceous materials, organic compounds, clay minerals, and metal oxides, which significantly modify the surface features of BCs (Mandal et al., 2016; Rajapaksha et al., 2016). The abovementioned composites work as a porous material to assist the dispersal of modifier/engineered agents within its matrix and increase the sorption capacity for various pollutants (Yao et al., 2014). In some cases, unwanted characteristics were reported during the composite formation, such as a decrease in the sorption capacity due to pore blockage/destruction (Zhang et al., 2013). Thus, it is necessary to assess the negative and positive effects of BC engineering on the sorption of pollutants. Previous studies comprehensively reviewed BC production and elucidated their characteristics and sorption capacities for different pollutants (Ahmad et al., 2014; Mohan et al., 2014; Liu et al., 2015; Inyang et al., 2016). However, less attention has been paid to modified/engineered BC for pollutants removal (Premarathna et al., 2019a; Li et al., 2019; Krasucka et al., 2020; Sakhiya et al., 2020; Shakoor et al., 2021; Yadav et al., 2021; Qiu et al., 2022; Siddiq et al., 2022) (Table 2). Thus, the overarching aim of this study is to fill the information gap surrounding raw and engineered BCs and their characteristics, application, mechanism, and adsorption capacities by revisiting the published literature within the last 15 years (2005–2020) (Figure 1). This review provides an exhaustive summary of using different BC-based composites/adsorbents for removing aquatic pollutants (antibiotics, heavy metals, and nutrients), mechanisms involved in the sorption process, and different factors affecting the sorption process that could help in the development of better and effective BC composites for the remediation of contaminated water.

Raw biochar (base of the adsorbents)

BC is a carbon-rich solid produced by heating biomass (Murtaza et al., 2021a). Generally, BC is produced through the thermal treatment of feedstocks/biomass, including agricultural waste, sludge, manure, food waste, forest residue, and municipal solid waste (Murtaza et al., 2020). Hydrothermal carbonization and pyrolysis are used as common methods to produce BC from carbonous materials. BC prepared in these ways largely depends on biomass type, reaction media, and pyrolysis conditions. Pyrolysis is the most frequently used process. Based on the heating rate, residence time, and pyrolysis temperature, the procedure can be categorized into

TABLE 1 Details of various pyrolysis mechanism conditions and product yield.

Pyrolysis route	Pyrolysis temperature (°C)	Residence time	Heating rate (°C/s)	Biochar yield	Reference
Slow pyrolysis	300–550	Hours to days, 5–30 min	0.1–0.8	10%–35%	Bridgwater (2012); Hornung (2014)
Intermediate	300–450	Seconds to minutes	3–500	25%–40%	Di Blasi (2008); Bridgwater (2012); Hornung (2014)
Flash/fast pyrolysis	300–1,000	Hours	<10	30%–60%	Bridgwater (2012); Hornung (2014); Ahmad et al. (2014)
Hydrothermal carbonization	180–250	Hours	<10	About 60%	Premarathna et al. (2019b)

fast and slow pyrolysis (Shakoor et al., 2021). Fast/flash pyrolysis involves rapid thermal treatment of feedstock with low moisture content over a very limited time, usually lasting seconds. The procedure is carried out at 800°C–1,200°C temperatures. Slow pyrolysis is a procedure carried out at 450°C–500°C temperatures when the feedstock is thermally treated for more than a few minutes (Amusat et al., 2021). The slow pyrolysis method is environmentally friendly because it releases less amount of toxic gases into the atmosphere. Due to such properties, BC production by slow pyrolysis is believed to be sustainable. BC manufactured by slow pyrolysis is described as a valuable material for the removal of several pollutants from wastewater and soil (Zhang et al., 2017).

Factors affecting attributes of biochar

The reaction conditions during the pyrolysis method are mostly accountable for BC production. Factors including temperature, feedstocks, heating rate, and particle size largely influence the BC characteristics. The comprehensive knowledge of analyzing BC characteristics is significant for determining the BC application. Different biomass from various sources, including agricultural waste, plant materials, solid wastes, and wood biomass, has been applied for BC production (Shaheen et al., 2019).

Feedstocks/biomass

The feedstock is pondered as a complex solid material (inorganic or organic) and a biological substance obtained from living or non-living organisms. The feedstock is categorized into two groups: woody and non-woody feedstock. Woody feedstocks consist of forest and tree resides (Tripathi et al., 2016). Woody feedstocks contain low ash and moisture contents, less voidage, high bulk density, and high calorific value (Jafri et al., 2018). Non-woody feedstock includes agricultural and industrial residue and animal waste. Non-woody feedstocks usually have high ash and moisture contents, higher voidage, low bulk density, and lower calorific value (Jafri et al., 2018). Among different feedstock characteristics, moisture content has a prominent effect on biomass creation. Excessive moisture content in biomass mainly inhibits the generation of char and increases the quantity of energy required to achieve the pyrolysis temperature (Jafri et al., 2018). Low moisture contents in the feedstock are preferred for BC production owing to the notable reduction in the heat energy and the decrease in the time required for the pyrolysis procedure, which makes BC production economically suitable compared with feedstock with higher moisture contents (Tomczyk et al., 2020). Generally, woody biomass has greater lignin, hemicellulose, and cellulose compared to biomass obtained from herbaceous species (Lupoi and Smith 2012). Nevertheless, apart from the lignin, hemicellulose, and cellulose, a high pyrolysis yield is also related to a high content of inorganic components of the feedstock, which is evident from relatively low volatile matter and higher ash content (Jafri et al., 2018). For instance, BCs obtained from woody biomass have lower ash content (<7%) than BCs produced from non-woody biomass (>50%). Mukome et al. (2013) found lower ash content in BC derived from eucalyptus compared to cow manure and poultry litter. BCs produced from grass and manure usually have a higher content of ash because of the existence of silica from soil pollution (Mukome et al., 2013). The lower ash content makes BC more tractable to incorporation and transportation into the soils, as there is less wind-blown loss (Mukome et al., 2013). Moreover, ash contents were the lowest in BC derived from woody biomass (1.5%–3%) and the highest in BCs produced from peanut shells (7%–12%). The selection of BCs obtained from woody biomass would limit the increase in soil ash content, which has been linked with enhanced hydrophobicity. Enhancement in hydrophobicity causes potential retention of hydrophobic agrochemicals, such as herbicides (Zhang et al., 2019). Various studies have exhibited that rigorous control of the feedstock materials and pyrolysis conditions facilitate a considerable reduction in the emission amounts of atmospheric pollutants such as dioxins and Polycyclic Aromatic Hydrocarbons (PAHs) and particulate matter accompanying BC production. The high lignin content in

TABLE 2 Published reviews based on the biochar application in the removal of various types of pollutants in water (2010–2022).

Review title	Pharmaceutics	Cations	Anions	PAHs	Agrochemicals	Dyes	Publishing journals	Reference
Engineered biochars for recovering phosphate and ammonium from wastewater: a review		√	√	√	√	√	Science of the Total Environment	Shakoor et al. (2021)
Engineered biochar – a sustainable solution for the removal of antibiotics from water	√	√	√	√			Chemical Engineering Journal	Krasucka et al. (2020)
Biochar for the removal of contaminants from soil and water: a review	√	√	√	√	√	√	Biochar	Qiu et al. (2022)
Preparation, modification and environmental application of biochar: a review		√	√	√	√	√	Journal of Cleaner Production	Wang & Wang (2019)
Engineered/designer biochar for contaminant removal/ immobilization from soil and water: potential and implication of biochar modification	√	√	√	√	√	√	Chemosphere	Rajapaksha et al. (2016)
Biochar technology in wastewater treatment: a critical review	√	√	√	√	√	√	Chemosphere	Xiang et al. (2020)
Biochar-assisted wastewater treatment and waste valorization	√	√	√	√	√	√	Applications of Biochar for Environmental Safety	Pokharel et al. (2020)
Removal of heavy metals from aqueous solution using carbon-based adsorbents: a review	√	√	√	√	√		Journal of Water Process Engineering	Duan et al. (2020)
Application of biochars in the remediation of chromium contamination: fabrication, mechanisms, and interfering species	√	√	√			√	Journal of Hazardous Materials	Zheng et al. (2020)
Biochar-based engineered composites for sorptive decontamination of water: a review	√	√	√	√	√		Chemical Engineering Journal	Premarathna et al. (2019a)
Organic and inorganic contaminants removal from water with biochar, a renewable, low cost and sustainable adsorbent—a critical review	√	√	√	√	√	√	Bioresource Technology	Mohan et al. (2014)
Progress in the preparation and application of modified biochar for improved contaminant removal from water and wastewater	√	√	√	√		√	Bioresource Technology	Ahmed et al. (2016)
Influences of feedstock sources and pyrolysis temperature on the properties of biochar and functionality as adsorbents: a meta-analysis	√	√	√	√	√		Science of The Total Environment	Hassan et al. (2020)
Biochar based removal of antibiotic sulfonamides and tetracyclines in aquatic environments: a critical review	√	√	√				Bioresource Technology	Peiris et al. (2017)
Production, activation, and applications of biochar in recent times.	√			√	√	√	Biochar	Sakhiya et al. (2020)

(Continued on following page)

TABLE 2 (*Continued*) Published reviews based on the biochar application in the removal of various types of pollutants in water (2010–2022).

Review title	Pharmaceutics	Cations	Anions	PAHs	Agrochemicals	Dyes	Publishing journals	Reference
Recent advances in engineered biochar productions and applications	√	√	√	√	√	√	Critical Reviews in Environmental Science and Technology	Wang et al. (2017a)
Biochar-based nanocomposites for the decontamination of wastewater: a review	√	√	√	√	√	√	Bioresource Technology	Tan et al. (2016a)
Preparation and application of magnetic biochar in water treatment: a critical review	√						Science of The Total Environment	Li et al. (2019)
Synthesis of magnetic biochar from agricultural waste biomass to enhancing route for wastewater and polymer application: a review	√	√	√	√		√	Renewable and Sustainable Energy Reviews	Thines et al. (2017)
A critical review on arsenic removal from water using biochar-based sorbents: the significance of modification and redox reactions		√	√	√	√		Chemical Engineering Journal	Amen et al. (2020)
Wood-based biochar for the removal of potentially toxic elements in water and wastewater: a critical review	√	√	√	√	√	√	International Materials Reviews	Shaheen et al. (2019)
Review of the use of activated biochar for energy and environmental applications	√	√	√	√	√	√	Carbon letters	Lee et al. (2018)
Removal of arsenic from water using nano adsorbents and challenges: a review		√	√	√	√		Journal of Environmental Management	Lata and Samadder (2016)
Review of organic and inorganic pollutants removal by biochar and biochar-based composites	√	√	√	√	√	√	Biochar	Liang et al. (2021)
Advances in decontamination of wastewater using biomass-based composites: a critical review	√	√	√	√	√	√	Science of The Total Environment	Yadav et al. (2021)
Biochar adsorbents for arsenic removal from water environment: a review		√	√	√			Bulletin of Environmental Contamination and Toxicology	Srivastav et al. (2021)
Removal of arsenic from contaminated groundwater using biochar: a technical review		√	√	√			International Journal of Environmental Science and Technology	Siddiq et al. (2022)
Biochar technology in wastewater treatment: a critical review	√	√	√	√	√	√	Chemosphere	Xiang et al. (2020)
Review of biochar properties and remediation of metal pollution of water and soil		√	√	√	√		Journal of Health and Pollution	Duwiejuah et al. (2020)
Modified adsorbents for removal of heavy metals from aqueous environment: a review		√	√	√	√	√	Earth Systems and Environment	Kumar et al. (2019)
Treatment of aqueous arsenic—a review of biochar modification methods		√	√	√			Science of The Total Environment	Benis et al. (2020)
Biochar as a sorbent for contaminant management in soil and water: a review	√	√	√	√	√	√	Chemosphere	Ahmad et al. (2014)

plant biomass has been stated to stimulate carbonization and improvement in BC ash and carbon contents (Zielinska et al., 2015).

Pyrolysis temperature

BC production process had three phases: pre-pyrolysis, post-pyrolysis, and the creation of carbonous products

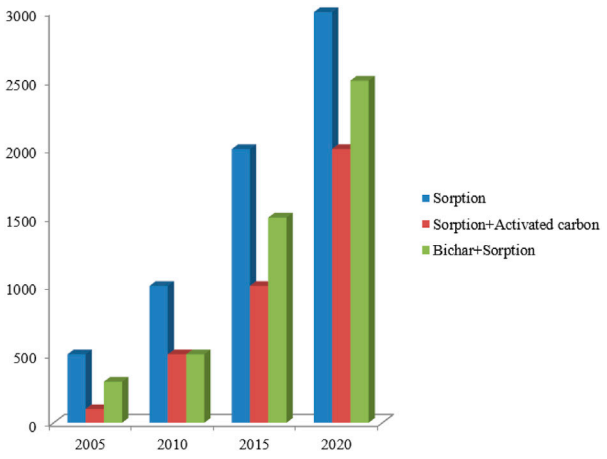

FIGURE 1
Science Citation Indexed publications on sorption and sorption related to biochar and activated carbon (2005–2020).

(Murtaza et al., 2022). The first phase (200°C) is accredited to the evaporation of light volatiles and moisture. The evaporation of moisture causes the breakage of bonds and the creation of hydroperoxide, -CO, and -COOH functional groups (Lee et al., 2017). In the second phase (200°C–500°C), cellulose and hemicelluloses are decomposed and devolatilized at a faster rate. In the last phase (beyond 500°C), the degradation of organic matter occurs, such as lignin with stronger chemical bonds (Ding et al., 2014). Pyrolysis temperature impacts the structure and physicochemical attributes of BC, such as functional groups, pore structure, elemental components, and surface area (Dhyani and Bhaskar, 2018). Higher pyrolysis temperature resulted in an elevation of carbonized fractions, surface area, volatile matter, and pH and a decrease in surface functional groups and CEC (Tomczyk et al., 2020). Additionally, ester groups, aliphatic alkyls, and exposure to aromatic lignin core under high temperatures may increase the surface area (Jayathilake et al., 2021). Ambaye et al. (2021) reported that at low temperatures/slow pyrolysis, lignin content is not converted into hydrophobic PAHs and BC develops more hydrophilic characteristics. In contrast, in fast pyrolysis (more than 600°C), BC gets thermally stable and develops a more hydrophobic character. Various amorphous C structures are also generated during the pyrolysis process because of cellulose degradation (Zhao et al., 2017). Furthermore, structural aromaticity enhances with an increase in pyrolysis temperature, which aids in improving resistance to microbial decomposition (Tomczyk et al., 2020). BC derived at fast pyrolysis was more efficient in removing inorganic and organic pollutants mainly due to its higher surface area and significant development of micropores (Amalina et al., 2022). In contrast, BC derived at low temperatures/slow pyrolysis showed more polymorphous organic characteristics owing to the presence of cellulose and aliphatic structures (Joseph et al., 2021).

Residence time

Increasing the residence time at low pyrolysis temperature (300°C) causes a small decrease in BC yield and a reformist increase in pH and iodine adsorption amount of BCs. In contrast, increasing residence time at high pyrolysis temperature (600°C) slightly influences BC pH or yield, but it reduces the iodine adsorption amount of BCs (Liang et al., 2016; Janu et al., 2021). Zhao et al. (2018) reported that the morphology and surface area were significantly affected by residence time, which is often overlooked in the literature. The influence of residence time on the *Brassica napus*-derived BC yield indicates a negative impact on brassica yield. A negative effect is logical as the greater mass would be volatilized during extended pyrolysis conditions. Nevertheless, the results show that residence time only slightly affects *Brassica napus*-derived BC yield, suggesting that a maximum pyrolysis yield can be achieved in a relatively short residence time (Zhao et al., 2018). Wang J. et al. (2020) found that pH reveals only a slightly positive correlation with increasing residence time. Zhao et al. (2018) found little effect of residence time on functional groups. The two adsorption peaks found at 1,425 and 865 cm^{-1} may be attributed to polycyclic aromatic structures and CH_2 addition, respectively, also displaying the peaks at 1,600 cm^{-1} for BC derived at residence times ranging 10–100 min, and less intense peaks at 865 cm^{-1}, which may be ascribed to aromatic CH out-of-plane deformation.

Surface functional groups

Heating to temperatures of 400°C–600°C rearranges and breaks the chemical bonds in the biomass, creating new functional groups such as pyrrole, pyridine, pyrone, ether, phenol, anhydride, chromene, quinine, lactol, lactone, and carboxyl (Mia et al., 2017). The key functional groups present at the BC surface that improve its sorption capacities include lactonic, amide, carboxylic, amine, and hydroxyl groups. The major factors that impact BC surface functional groups are temperature and feedstock (Li H. et al., 2017; Murtaza et al., 2021c). Additionally, when other attributes, such as porosity, surface area, and pH, increase, there is a chance of a decrease in the char functional groups. BC manufactured at various temperatures exhibited a substantial alteration in their surface functional groups (Li M. et al., 2017). Surface functional groups can act as electron donors–electron acceptors, stimulating the generation of co-existing areas. Their traits can range from acidic to basic and concert hydrophilic to hydrophobic. BCs are derived from agricultural biomass by pyrolysis, mainly involving the cleavage of O-alkylated carbons and anomeric O-C-O carbons in addition to the

production of fused-ring aromatic structures and aromatic C-O groups. With increasing pyrolysis, the mass cleavage of O-alkylated groups and anomeric O-C-O carbons occurred prior to the production of fused-ring aromatic structures (Joseph et al., 2021). Xiao et al. (2018) presented that the leading functional groups of BC are heterocyclic and aromatic C, which are supposed to be stable in soil owing to their chemical resistance.

Ash and carbon content

The ash and carbon contents of BC enhance with increasing preparation temperature (Fuertes et al., 2010). Higher carbon content proposes that BCs probably still comprise a certain quantity of original organic plant waste, for example, cellulose (Chen et al., 2008). Rafiq et al. (2016) described that fast pyrolysis caused an enhancement of ash content (5%–18%). Enhancement in P, K, Ca, and Mg on BCs prepared at higher temperatures is due to increased ash content (Zama et al., 2017). Enhanced carbon content (62%–92%) with a rise in prepared temperature occurs due to a higher level of polymerization, contributing to a more condensed carbon structure in BC (Domingues et al., 2017). BCs with higher ash contents also tend to have larger amounts of trace metals and PAHs (Yargicoglu et al., 2015).

Pyrolysis conditions have a significant effect on the ash and carbon contents. For instance, the C content (56%–68%) of BC derived from orange peel increased with increasing production temperature (Tag et al., 2016). Carbon contents (27%–35%) of BC derived from poultry litter are reduced with increasing manufactured temperatures (Tomczyk et al., 2019). The carbon contents in various BCs exposed the trend of natural plants (88%) > crops residues (74%) > forest residues (23%). With increasing the pyrolysis temperature, the volatile matter and moisture contents in biomass are gradually reduced, whereas the contents of ash in BCs per unit mass are enhanced. The ash content ranged 22%–32% in BC derived from apricot at 300°C and 600°C, which was the highest among eight kinds of feedstocks. The lowest ash content was found in pinewood BC (1.7%–4.9%). Rice husk and peanut shell BCs ranked second and third in terms of ash content, respectively (Qi et al., 2022).

Overall, the quality and yield of BC are primarily influenced by feedstock, temperature, heating rate, and particle size, as they directly affect the BC characteristics. Therefore, the process needs careful management to obtain consistent yield and quality of BC. The selection of a suitable feedstock is the first step in BC production. Usually, two types of feedstocks (i.e., woody and non-woody) are used in BC production. Among different feedstock characteristics, moisture content has a prominent effect on biomass creation. Feedstock containing low moisture content is preferred in BC production due to the considerable reduction in the heat energy and time required for the pyrolysis procedure. It makes BC production economically suitable compared to feedstock with higher moisture contents.

Pyrolysis temperatures considerably impact the structure and physicochemical attributes of BC. BC derived at fast pyrolysis was more efficient in removing inorganic and organic pollutants mainly due to its higher surface area and significant development of micropores, whereas BC derived at low temperatures (slow pyrolysis) showed more polymorphous organic characteristics due to cellulose and aliphatic structures. Residence time is also an important factor that needs to be considered in the pyrolysis process. Increasing the residence time at low pyrolysis temperature (300°C) causes a small decrease in BC yield and a reformist increase in pH and iodine adsorption amount of BC. In contrast, increasing residence time at high pyrolysis temperature (600°C) slightly influenced BC pH and yield, but it reduced the iodine adsorption amount of BC.

The BC manufactured at different temperatures substantially altered their surface functional groups. Biomass heating at temperatures of 400°C–600°C breaks and rearranges the chemical bonds in the biomass, producing new functional groups. BC produced at high temperatures (600°C–700°C) contains a highly hydrophobic nature with well-organized C layers, but they possess lower contents of H- and O-containing functional groups due to dehydration and deoxygenation of the biomass. In contrast, BC produced at lower temperatures (300°C–400°C) displays a more diversified organic character due to aliphatic and cellulose-type structures. The BC carbon and ash contents increase with increasing pyrolysis temperature. It is found that increased pyrolysis temperature causes an increase of 5.7%–18.7% in ash contents. The increase in the ash content resulted from a progressive concentration of inorganic constituents and organic matter combustion residues. Increased carbon content (62.2%–92.4%) with an increase in pyrolysis temperature occurs due to a higher degree of polymerization, leading to a more condensed carbon structure in the BC. A clear understanding of the abovementioned factors is essential for preparing a better and more effective BC product that could provide substantial long-term benefits.

Sorption characteristics of biochar

Recently, BC applications have focused on eliminating various pollutants from water. BC fabricated at fast pyrolysis (500°C–700°C) shows higher sorption efficiency for antibiotics and trace/heavy metals compared to the BC prepared at slow pyrolysis (250°C–400°C) (Shen et al., 2017). The higher aromaticity of fast pyrolysis-based BCs enhances the removal potential of antibiotics and trace metals, and at the same time, the reduction in polarity at higher temperatures supports the same (Rajapaksha et al., 2015). Adsorption of

trichloroethylene mainly occurs through hydrophobic partitioning and pore-filling mechanisms (Ahmad et al., 2013). Trichloroethylene adsorption is prevented by O-enriched functional groups, thus leaving behind intact BC produced at high temperatures, which otherwise adsorb water by H-bonding (Chen et al., 2008). Generally, antibiotics interact with BC by H-bonding, electrostatic attraction, and Van der Waals interactions (Solanki and Boyer, 2017). A large number of functional groups in BC are generated at low temperatures; their processes of sorption are mainly explained by H-bonding and electrostatic attraction between BC functional groups and molecules of pollutants (Tan et al., 2016b). BCs produced at higher temperatures retain a higher amount of anionic dyes and a lower amount of cationic dyes. Sorption of anionic and cationic dyes occurred by π–π interactions and cation exchange, respectively (Yang G. et al., 2016). Adsorption efficiency for pesticides was also improved by increasing the production temperature. Pesticides interact with BC by the formation of the amide bond, hydrophobic interactions, van der Waals forces, H-bonding, ionic bonding, covalent bond, electrophilic addition, base–acid interactions, and strong π–π EDA interactions (Li Y. et al., 2017). Sorption of both inorganic and organic pollutants *via* BC is pH-dependent because the surface charge of BC varies according to the pH_{pzc} of BC. At pH < pH_{pzc}, the surface has a more negative charge, which accelerates the removal of positively charged pollutants owing to the electrostatic attraction. At pH > pH_{pzc}, a surface with a positive charge inhibits the sorption of positively charged contaminants because of electrostatic repulsion (Gao et al., 2015). Pesticides, antibiotics, and other organic contaminants show different pKa values. Hence, contingent on the pH of a solution, the antibiotic can mainly exist in its neutral, anionic, and cationic forms (Chang et al., 2014). At high pH values, anionic species become the prevailing form of some antibiotics, including ciprofloxacin, sulfamethazine, and tetracycline. The electrostatic repulsion between anionic species of antibiotics and BC negatively charged surface would consequently result in reduced sorption at high pH (Han et al., 2013). Nonetheless, higher pH values also accelerate weaker π–π EDA interactions between the BC surface and the antibiotic (Han et al., 2013). At low pH values, anionic dye sorption mainly happens by electrostatic attraction between protonated carboxylic and hydroxyl acid groups of BC and negatively charged anionic dye (Vimonses et al., 2009). Nonetheless, cationic dye adsorption decreases owing to repulsive forces occurring between positively charged functional groups of BC and cationic dyes (Yang X. et al., 2016). At high pH values, the protonated BC functional groups increasingly deprotonated, and as a result, electrostatic interaction weakens, reducing the anionic dyes sorption but causing an increase in sorption amount for the cationic dyes (Yang G. et al., 2016).

Biochar-based engineered composites: synthesis methods

This section mainly emphasizes the synthesis methods of various key BC composites (Figure 2).

Biochar composite preparation with metals and metal oxides

Generally, coating with metal and metal oxides (chlorides and nitrates) is performed *via* soaking BCs in the solution of metal and metal oxides. The most commonly used agents for modification stated in the literature are $MgCl_2$, Fe $(NO_3)_3$, Fe_2O_3, and $FeCl_3$ (Fristak et al., 2017; Ooi et al., 2017). In BC–metal and metal oxide composites, BC acts as a porous C platform upon which metal oxides precipitate, therefore improving the surface area for the sorption (Fristak et al., 2017). Synthesis of metal oxide–BC composites was done in two ways: 1) pre-pyrolysis modification and impregnation of the feedstock followed through pyrolysis and 2) post-pyrolysis modification and pyrolysis of the biomass followed by soaking in a solution of metal ion (Ahmed et al., 2016). In the process of pre-pyrolysis, the feedstock is immersed in a metal salt solution and then pyrolyzed under a low-oxygen environment. In the process of post-pyrolysis, pyrolyzed biomass is immersed in a metal salt solution (Zhang et al., 2012; Wang M. C. et al., 2015; Ooi et al., 2017).

Synthesis of clay mineral-based biochar composites

Recently, clay minerals have been extensively used in agriculture, pharmacy, and medicine, as well as the synthesizing of ink, cosmetics, and paint (Pusch, 2015). Due to their great ion-exchange capabilities, higher high surface area, and lamellar structures, clay minerals have been efficiently utilized as adsorbents to eliminate various types of metalloids/heavy metals, polymers, and antibiotics (Rajapaksha et al., 2011; Aristilde et al., 2016). Nonetheless, the sole application of clays as adsorbents lacks potential due to the re-generation problems and amount of residue after sorption. Composites of clay–BC synthesized *via* mixing various amounts of clay with BC have exhibited favorable results and great sorption capacities in eliminating different pollutants (Yao et al., 2014). Although several approaches have been applied to create BC–clay composites, the most common ones include the production of BC–clay slurry for pyrolysis (Yao et al., 2014). Briefly, the biomass is immersed in a suspension of clay produced by mixing the powdered material with distilled water and pyrolyzed under an oxygen-limited environment in a muffle furnace at the appropriate temperature (Yao et al., 2014). In

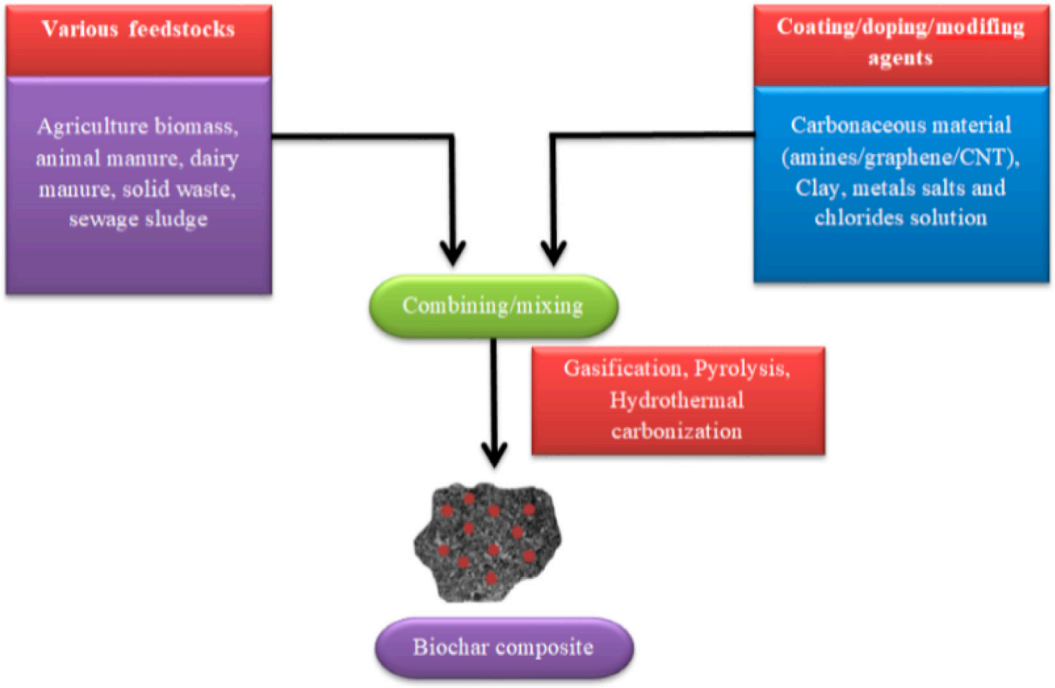

FIGURE 2
Engineered/modified composite synthesis pathways.

contrast, BC can be directly dipped in slurry produced with clay minerals, acetic acid, and distilled water; stirred overnight, and then dried at 60°C in an oven for 24 h. The most commonly used weight ratios of clay: BC for procedures was 1:1, 1:2, 1:4, and 1:5 (Zhang et al., 2012; Yao et al., 2014).

Biochar composite preparation with carbonaceous materials

Engineering/modification of BCs via carbonaceous materials (containing functional groups), can generate strong bonds with both BC surface and contaminants present in the water (Zhou et al., 2014). Generally, CNT, amines, graphene, and polysaccharides are the most commonly used agents for modification (Sarkar et al., 2018). Such treatment/coating can be attained either by a simple chemical reaction or through mixing BC with polymers enriched in amino groups, such as chitosan or polyethyleneimine (Zhou et al., 2013). Among carbonaceous materials, CNT and graphene are commonly applied in composite production owing to their strong binding affinity through functionalization with -COOH and -OH groups by chemical oxidation process (Liu et al., 2016). Due to the higher surface area and porous structure of BCs, they can be utilized as a host to stabilize and distribute nanomaterials and increase the range of applications (Liu et al., 2015). Modification/engineering can further improve the sorption capacities of BCs against different contaminants (Zhou et al., 2014).

Biochar composite characteristics and influencing factors

BC composites are synthesized by adding different materials such as CNT, graphene, clay and metal salts, nitrates, and oxide solutions with feedstock. For BC production, various feedstocks from a range of carbonaceous and agricultural materials have been employed (Lehmann and Joseph, 2009). The properties of BC composites largely depend on pyrolysis conditions, feedstock characteristics, and doping/coating or mixing agents (Rajapaksha et al., 2016). Table 3 summarizes the properties of BC composites produced from several feedstocks under different pyrolysis temperatures. The elemental contents and yield of BC composites are reduced with raising pyrolysis temperature owing to a higher loss of volatile elements (Rawal et al., 2016). Thus, carbonaceous materials, metal oxides, and clay mineral modifiers strongly impact the BC yield (Rawal et al., 2016). The BC ash content positively correlates with pyrolysis temperatures (Gai et al., 2014). The content of ash also varied with the kinds of feedstock biomass. Thus, both clay and metal oxide modifications marginally increase the ash content in the

TABLE 3 Properties of engineered biochar-based composite synthesized from various feedstocks.

Biochar feedstock	Modifier agent	Pyrolysis temperature	Pyrolysis time	Yield (%)	pH	C	H	O	N	S	Ca	Al	Fe	Mg	K	Ash	SSA m^2g^{-1}	Pore volume cm^3g^{-1}	Reference
Potato stem	Unmodified	500	6 h	14.89	10.40	75.81	—	19.30	—	—	1.51	0.39	—	1.49	—	24.67	99.43	0.08	Rawal et al. (2016)
	Attapulgite- modified			30.71	9.93	59.75	—	30.92	—	—	2.13	1.15	—	2.05	—	50.33	90.40	0.12	
Pistachio shells	Unmodified	400	1 h	31.40	6.40	73.42	2.93	23.44	0.74	—	—	—	—	—	—	—	572.4	—	Komnitsas and Zaharaki (2016)
	$FeCl_3$-modified			—	6.10	78.24	3.07	17.95	0.71	—	—	—	—	—	—	—	421.5	—	
Paper waste	Unmodified	750	2 h		8.46	—	—	—	—	—	—	0.30				36.20	174	40	Chaukura et al. (2017)
	Fe_2O_3-modified				2.86	—	—	—	—	—	—	22.60				49.30	15.30	3.50	
Wheat straw	Unmodified	600	1 h	27.90	6.90	—	—	—	—	—	—	—	—	—	—	—	4.50	0.01	Tang et al. (2015)
	Graphene-modified (1%)			29	7.10	—	—	—	—	—	—	—	—	—	—	—	17.30	0.12	
	Graphene-modified (0.5%)			27.70	6.70	—	—	—	—	—	—	—	—	—	—	—	15.80	0.06	
	Graphene-modified (0.1%)			25.70	6.40	—	—	—	—	—	—	—	—	—	—	—	10.90	0.03	
Sawdust	Unmodified	400	1 h	17.70	4.80	65.20	2.19	24.52	0.39	—	—	—	—	—	—	—	124.60	—	Komnitsas and Zaharaki (2016)
	$FeCl_3$-modified			—	4.60	72.90	2.11	30.23	0.36	—	—	—	—	—	—	—	110.80	—	
Pecan shells	Unmodified	400	1 h	34.70	6.10	71.60	2.75	25.15	0.60	—	—	—	—	—	—	1.80	142.40	—	Komnitsas and Zaharaki (2016)
	$FeCl_3$-modified			—	5.60	65.20	2.63	23.85	0.72	—	—	—	—	—	—	—	397.30	—	
Corncob	Unmodified	500	2 h	—	8.74	82.84	2.11	—	1.36	—	—	—	—	—	—	16.27	16.50	—	Fristak et al. (2017)
	$FeNO_3)_3$-modified			—	3.38	74.56	1.61	—	2.42	—	—	—	—	—	—	14.18	6.19	—	
Pinewood	Unmodified	600	1 h	—	—	85.70	2.10	11.40	0.30	—	0.19	0.04	0.02	0.05	0.12	—	209.60	—	Wang M. C. et al. (2015)
	Hematite-modified			—	—	51.70	1.40	43.10	0.20	—	0.10	0.24	2.95	0.04	0.14	—	193.10	—	
Bamboo bagasse	Unmodified	600	1 h	—	—	80.89	2.43	14.86	0.15	—	0.34	0.04	0.04	0.23	0.52	—	375.5	—	Yao et al. (2014)
	Montmorillonite-modified			—	—	81.81	2.17	14.02	0.73		0.82	0.01	0.01	0.13	0.24	—	401	—	
Hickory chip	Unmodified	600	1 h	—	—	76.45	2.93	18.32	0.79	—	0.91	0.11	0.05	0.21	0.15	—	388.3	—	
	Montmorillonite-modified			—	—	83.25	2.26	12.41	0.25	—	0.21	0.68	0.23	0.14	0.33	—	408.1	—	
Bamboo	Unmodified iron kaolinite-modified	250	30 min	78	—	51.90	5.45	—	0.87	0.08	0.50	—	0.01	—	0.83	14.38	—	0.36	Rawal et al. (2016)
				86	—	48.70	5.15	—	0.50	1	0.05	0.03	2	—	0.74	15.43	—	0.73	
Bamboo	Unmodified	250	30 min	78	—	51.90	5.45	—	0.87	0.08	0.50	—	0.01	—	0.83	14.38	—	0.36	Rawal et al. (2016)
	Iron bentonite-modified			76	—	48.70	5.15	—	0.50	0.73	0.05	0.01	1.20	—	0.35	15.91	—	0.88	
Bamboo	Unmodified	350	30 min	60	—	71.50	4.02	—	1.11	0.07	0.08	—	0.01	—	1.40	28.08	—	1.05	Rawal et al. (2016)
	Iron kaolinite-modified			59	—	67.60	3.30	—	0.87	1.10	0.05	0.04	2.10	—	1	11.40	—	0.86	
Bamboo	Unmodified	350	30 min	60	—	71.50	4.02	—	1.11	0.07	0.08	—	0.01	—	1.40	28.08	—	1.05	Rawal et al. (2016)

(Continued on following page)

10.3389/fenvs.2022.1035865

TABLE 3 (*Continued*) Properties of engineered biochar-based composite synthesized from various feedstocks.

Biochar feedstock	Modifier agent	Pyrolysis temperature	Pyrolysis time	Yield (%)	pH	C	H	O	N	S	Ca	Al	Fe	Mg	K	Ash	SSA m^2g^{-1}	Pore volume cm^3g^{-1}	Reference
	Iron bentonite-modified			63	—	57.20	3.51	—	0.80	1.40	0.12	0.03	2.50	—	2.82	24.14	—	0.77	
Bamboo	Unmodified	450	30 min	35	—	75	3.42	—	1.38	0.12	0.10	0.01	0.02	—	1.40	19.10	—	0.77	Rawal et al. (2016)
	Iron kaolinite-modified			48	—	62.90	2.82	—	1.45	1.10	0.07	0.09	2.90	—	1.20	35.60	—	0.56	
Bamboo	Unmodified	450	30 min	35	—	75	3.42	—	1.38	0.12	0.10	0.01	0.02	—	1.40	19.10	—	0.77	Rawal et al. (2016)
	Iron bentonite-modified			42	—	61	2.79	—	0.84	1.30	0.12	0.03	2.50	—	0.63	56.87	—	0.73	
Bamboo	Unmodified	550	30 min	33	—	79.20	2.72	—	1.28	0.06	0.08	0.01	0.03	—	0.85	26.34	—	1.01	Rawal et al. (2016)
	Iron kaolinite-modified			38	—	63.60	1.72	—	1.39	0.52	0.05	0.16	2.30	—	0.64	14.61	—	0.16	
Bamboo	Unmodified	550	30 min	33	—	79.20	2.72	—	1.28	0.06	0.08	0.01	0.03	—	0.85	26.34	—	1.01	Rawal et al. (2016)
	Iron bentonite-modified			38	—	70.20	2.49	—	0.79	0.63	0.10	0.10	1.70	—	0.37	31.64	—	0.42	
Date palm leaves	Unmodified	300	4 h	—	—	48.97	5.28	31.16	2.89	0.56	—	—	—	—	—	8	—	—	Kirmizakis et al. (2022)
	$Fe(NO_3)_3$-modified			79	—	50.19	2.80	33.51	1.80	0.26	—	—	—	—	—	11.7	—	—	
Date palm leaves	Unmodified	300	4 h	—	—	48.97	5.28	31.16	2.89	0.56	—	—	—	—	—	8	—	—	Kirmizakis et al. (2022)
	$Fe(NO_3)_3$-modified			48	—	55.40	1.12	30.95	1.12	0.0	—	—	—	—	—	26	—	—	
Poplar	Unmodified	600	2 h	—	—	—	—	—	—	—	—	—	—	—	—	—	7.37	0.018	Xu et al. (2020)
	$FeCl_3$-modified			—	—	—	—	—	—	—	—	—	—	—	—	—	21.25	0.021	
Poplar	Unmodified	900	2 h	—	—	—	—	—	—	—	—	—	—	—	—	—	7.37	0.018	Xu et al. (2020)
	$FeCl_3$-modified			—	—	—	—	—	—	—	—	—	—	—	—	—	2.88.53	0.11	
Wheat straw	Unmodified	650	3 h	—	10.6	54	1.8	11	0.9	—	—	—	—	—	—	32.3	26.3	0.026	Godlewska et al. (2020)
	$Fe(NO_3)_3$-modified			—	2.80	46	1.6	17.50	2.6	—	—	—	—	—	—	32.3	22.5	0.029	
Coconut shell	Unmodified	700	1 h	—	—	81.42	1.84	7.74	0								650.8	0.3804	Sun et al. (2022)
	$FeCl_3$-modified			—	—	90.86	1.10	8.13	1.01								624	0.3300	
Sludge biochar	Unmodified	500	2 h	—	—	—	—	—	—	—	—	—	—	—	—	—	14	2.97	Ma et al. (2020)
	Zn/Fe-modified			—	—	—	—	—	—	—	—	—	—	—	—	—	41.6	1.11	
Cornstalk	Unmodified	500	1.5 h	—	9.48	—	—	—	—	—	—	—	—	—	—	—	760.7	0.3698	Wang et al. (2017b)
	Υ-Fe_2O_3-modified			-	8.53	—	—	—	—	—	—	—	—	—	—	—	856.8	0.4007	
Reed straw	Unmodified	500	5 h	33.32	—	33.19	—	38.46	4.66	0.44	0.70	0.35	—	—	—	—	159.86	0.0882	Yang et al. (2019)
	Hematite-modified			45.13	—	56.41	—	26.31	4.58	6.65	0.03	0.19	—	—	—	—	54.33	0.0532	
Grapefruit peel	Unmodified	400	2 h	—	10.13	72.32	—	20.02	2.52	—	—	—	0.43	—	—	—	1.706	0.003	Wang K. et al. (2020)
	Υ-Fe_2O_3-modified			—	7.96	41.57	—	38.11	1.64	—	—	—	18.05	—	—	—	20.732	0.110	

10.3389/fenvs.2022.1035865

BC composites compared to pristine BC owing to the thermal stability of clay minerals and metal oxide (Chaukura et al., 2017; Chen et al., 2017; Li H. et al., 2017). A slight reduction in the carbon content of BC composites subsequent to clay and metal treatment may occur due to the introduction of metallic components (Li M. et al., 2017). For example, some components in modifier agents may act as catalysts that result in several pollutant degradation processes. Nonetheless, pyrolysis temperature and feedstock are the leading factors determining carbon content. At higher temperatures, carbon content increases owing to high dehydrogenation and carbonization and a great amount of carbon available within aromatic structures (Novak et al., 2009; Rawal et al., 2016). Higher carbon contents in biomass prepare BC composites with high carbon contents owing to the insufficient quantity of hydrogen in its structural matrix (Lian et al., 2011). BC composite pH can be changed, rendering to the basicity or acidity of the doping/coating material (Chen et al., 2017). BC modification with clay minerals can change the content of oxygen and may introduce a large number of oxygen-enriched functional groups on the BC surface (Komnitsas and Zaharaki, 2016). Moreover, surface functional groups ascertain the surface basicity or acidity, which is a vital factor influencing the sorption capabilities and the selectivity of BC composites. Various clay minerals used in BC composites mostly consist of metals, including Si, Zn, Fe, Mg, Al, Na, and Ca (Nazir et al., 2016). Therefore, higher concentrations of metal exist in clay–BC composites compared to raw/pristine BC (Yao et al., 2014; Wang S. et al., 2015; Li Y. et al., 2017). Treatment by metal oxides raises the soluble salt within composites, hence increasing the electrical conductivity of BC composites (Fristak et al., 2017). Clay-coated BC shows higher thermal stability than unmodified BC (Yao et al., 2014). Furthermore, the modification of BC with carbonaceous materials shows higher thermal stability compared to unmodified BC (Zhou et al., 2014; Tang et al., 2015). If the modifier agent has magnetic features, the BC composite may show perpetual magnetic characteristics after pyrolysis (Zhou et al., 2014). Conversely, modification increases the surface area and sorption capacity of BC composite but reduces the surface area if pores are blocked due to excessive loading/coating (Fristak et al., 2017). Modification, increased residence time, and pyrolysis temperature also increase pore size, pore volume, and surface area of BC owing to the thermal demolition of oxygen- and hydrogen-enriched functional groups such as phenolic, ester, and aliphatic alkyl.

Sorption of antibiotics *via* biochar-based engineered composites

BC composites are the most complex group of BC adsorbents used for removing antibiotics. Table 4 summarizes the influence of the BC composite with clay minerals, carbonaceous materials, and metal oxides on removing antibiotics from water. Premarathna et al. (2019b) modified the municipal solid waste BC with clay minerals, including red earth and montmorillonite (by a pre-treatment technique). They used the prepared composite for the adsorption of tetracycline in a pH range of 3–9. Mixing red earth and montmorillonite minerals enhanced the surface area of the produced BC composites, indicating the lack of a pore-blocking process after the incorporation of the porous particles of the minerals into BC. However, the tetracycline removal amount did not differ substantially between pristine BC and red earth clay-modified BC. It was presented that tetracycline is primarily adsorbed by ion exchange, electrostatic attraction, H-bonding, π–π interactions, and chemisorption mechanisms (Premarathna et al., 2019a). Adsorption was dependent on solution pH. For BC-red earth clay composite and pristine BC, the tetracycline adsorption was not higher at low pH, resulting from electrostatic repulsion between the positively charged surface of the BCs and the positively charged tetracycline molecules. The maximum amount of tetracycline adsorption onto BCs was achieved at 5 and 7 pH, at which the antibiotic molecule is neutral (Premarathna et al., 2019b). The montmorillonite–BC composite showed a much higher (by approximately 20 times) adsorption capacity of tetracycline than the other two used adsorbents. This was due to the layered structure of montmorillonite that red earth clay does not own. The montmorillonite structure enabled the intercalation of antibiotics between the layers of BC, coupled with pore-filling (Premarathna et al., 2019a). For montmorillonite–BC composite, sorption was also efficient at low pH <4 (Premarathna et al., 2019b). Zhang et al. (2018) reported that the significantly increased removal capacity of norfloxacin after using montmorillonite–BC composite was much higher than the untreated BC. Due to the composite's higher porosity, the adsorption mechanism was associated with pore-filling. Electrostatic interactions and H-bonding also contributed to the adsorption mechanism, which was linked to enhancing the amount of O-enriched surface functional groups in the montmorillonite-containing composite and amphoteric structure of norfloxacin molecule (Zhang et al., 2018). The maximum sorption occurred at 5 and 11 pH, at which pH values of the antibiotic molecule are neutral (Zhang et al., 2018). Dissolved humic acid and Cu^{2+} ion presence in the solution reduced norfloxacin adsorption due to competition (Zhang et al., 2018). Ashiq et al. (2019) examined the ciprofloxacin sorption onto the bentonite–BC composite produced from municipal waste. They reported a 40% enhancement in ciprofloxacin sorption onto bentonite–BC composite, compared with raw BC (Ashiq et al., 2019). This enhancement was associated with the higher porosity of the composite-containing bentonite and the occurrence of electrostatic attraction between the ciprofloxacin molecule and

TABLE 4 Modified/engineered biochar used to remove antibiotics from the water.

Biochar	Modify agent	Pyrolysis temperature (°C)	Pyrolysis time	Pollutant	Enhancement in adsorption	Involved mechanism	Reference
Potato stem	Attapulgite	500	6 h	Norfloxacin	Adsorption ability was 1.7 times greater than pristine biochar. Around 80% of norfloxacin was removed	EDA, H-bonding, and pore-filling	Li H. et al. (2017)
Coconut shell	$FeCl_3$	700	1 h	Sulfadiazine	Adsorption capacity observed at 294.12 mg g^{-1}, higher than pristine biochar	Electron donor–acceptor, H-bonding	Sun et al. (2022)
Coconut shell	$FeCl_3$	700	1 h	Sulfamethazine	400 mg g^{-1} adsorption capacity noticed	Hydrophobic interactions, electrostatic interaction	Sun et al. (2022)
Coconut shell	$FeCl_3$	700	1 h	Sulfamethoxazole	Adsorption capacity was 454.55 mg g^{-1}, 7 times higher than raw biochar	EDA, H-bonding and pore-filling, and van der Waals forces	Sun et al. (2022)
Corn husk	Iron(III) chloride hexahydrate	300	1 h	Levofloxacin and tetracycline	Modified biochars showed higher sorption capacity for levofloxacin and tetracycline	F-replacement, H-bonding, and electrostatic attraction	Chen et al. (2019)
Poplar wood	Mixture $CaCl_2/FeCl_3$	700 and 900	1 h	Norfloxacin	Adsorption capacity up to 38.77 mg g^{-1}	Pore-filling and electron donor–acceptor	Liang et al. (2022)
Sludge biochar	Zn/Fe	500	2 h	Fluoroquinolones	Higher adsorption capacity of 83.7 mg g^{-1} was greater than unmodified biochar	H-bonding, electrostatic attraction, and pore-filling	Ma et al. (2020)
Cornstalk	ϒ-Fe_2O_3	500	1.5 h	Norfloxacin	Adsorption capacity was 7.62 mg g^{-1}	Electron donor–acceptor, H-bonding	Wang et al. (2017a)
Reed straw	Hematite	500	5 h	Norfloxacin	Adsorption capacity of norfloxacin was significantly increased using modified biochar	Ion exchange interaction and electron donor–acceptor	Yang et al. (2019)
Grapefruit peel	ϒ-Fe_2O_3	400	2 h	Norfloxacin	Adsorption amount was 61.43%, much higher than pristine biochar	Hydrogen bond and cation exchange	Wang L. et al. (2020)
Sawdust	Fe/Zn	600	2 h	Tetracycline	Removal capacity was higher than other untreated biochars	Chemisorption and electron donor–acceptor	Zhou et al. (2017)
Municipal solid waste	Bentonite	450	30 min	Ciprofloxacin	Modified biochar exhibited high removal capacity (190 mg/g), 40% higher than raw biochar	Electrostatic interactions, hydrogen bond, and cation exchange	Ashiq et al. (2019)
Eucalyptus globulus	nZVI	380	2 h	Chloramphenicol	Observed sorption was 70.5%	Electrostatic attraction and pore-filling	Ahmed et al. (2017)
sludge	Fe_3O_4	500	3 h	Tetracycline	The adsorption rate was 94.3%	Ion exchange interaction and electron donor–acceptor	Sun et al. (2021)
Reed	Magnetic composite	600	2 h	Florfenicol	Adsorption capacity of modified biochar for drug was 5.3 mg g^{-1}, higher than the pristine biochar (2.6 mg g^{-1})	EDA interaction, pore-filling, and H-bonding	Zhao and Lang (2018)
Crab shell	Ca	800	2 h	Chlortetracycline hydrochloride	Adsorption capacity was 1,975 mg g^{-1}, 10 times higher than raw biochar	H-bonding, electrostatic attraction, and cation bridging	Xue et al. (2016)
Peanut shell	Magnetic composite	800	1 h	Trichloroethylene	Adsorption capacity of modified biochar for drug was 4.6 mg g^{-1}	Reductive degradation, pore-filling, and hydrophobic partitioning	Liu et al. (2019)
Sawdust	Graphene oxide	600	2 h	Sulfamethazine	Adsorption amount was 6.5 mg g^{-1} using graphene oxide doped biochar, higher than other unmodified used biochar	Electrostatic attraction, H-bonding, cation exchange, pore-filling, and EDA interaction	Huang et al. (2017)

(Continued on following page)

TABLE 4 (*Continued*) Modified/engineered biochar used to remove antibiotics from the water.

Biochar	Modify agent	Pyrolysis temperature (°C)	Pyrolysis time	Pollutant	Enhancement in adsorption	Involved mechanism	Reference
Reed straw	TiO_2	500	6 h	Sulfamethoxazole	Removal capacity of engineered biochar was less than unmodified biochar	TiO_2-modified biochar structure supported the photo-catalytic activity of TiO_2	Zhang et al. (2017)

functional groups present on the adsorbent surface (Ashiq et al., 2019). Huang et al. (2017) examined the sulfamethazine adsorption onto the BC–graphene composite. The adsorption capacity was higher after using composite compared to pristine BC. Graphene loading increased the number of O-enriched functional groups on the adsorbent surface and surface area, contributing to the increase in sulfamethazine sorption (Huang et al., 2017). Sulfamethazine was exposed to undergo the chemisorption mechanism, with the dominant involvement of π–π EDA interactions (Huang et al., 2017). Sorption was examined in solutions with ionic strengths and different pH values. The antibiotic adsorption improved by reducing the solution ionic strength and was higher for solutions at 3 and 6 pH, at which the sulfamethazine molecule is electrically neutral (Huang et al., 2017). Inyang et al. (2015) conducted a study on the sorption of sulfamethazine onto BC composites with CNT. In order to synthesize BC composites, sugarcane bagasse and hickory chips were employed in two pre-treatment methods: 1) with a CNT suspension or 2) with a CNT suspension comprising a surfactant ($C_{18}H_{29}NaO_3S$). The addition of nanotubes markedly increased the sulfamethazine sorption capacity of both BCs. Maximum sulfamethazine sorption was attained with composites synthesized in the presence of surfactants, such as 56 and 86%, respectively. Simultaneously, the composite/engineered BCs for which the highest capacity was achieved were characterized by the lowest pH, indicating more participation of acidic groups that may have contributed to sulfamethazine binding (Inyang et al., 2015). In the case of BC composites produced from the CNT suspension with surfactant ($C_{18}H_{29}NaO_3S$) and sugarcane bagasse, as well as CNT suspension, a more than 40-fold enhancement in surface area was noticed relative to raw sugarcane bagasse BC. A similar result was not found for the hickory chip–BC composites. A study of the isotherms and kinetics of the sulfamethazine sorption onto the BC-based composites exhibited the antibiotic binding by π–π EDA interactions and chemisorption mechanism (Inyang et al., 2015). Yang G. et al. (2016) investigated the adsorption of tetracycline onto Fe–BC composite and pristine BC obtained from sewage sludge. The biomass was soaked in iron sulfate solution before pyrolysis (used pre-treatment method). The Fe–BC composite increased by 300% in tetracycline sorption capacity, much higher than pristine BC. It could be attributed to higher porosity and hydrophilicity induced by Fe loading. The study showed metal complexation and H-bonding with Fe-O groups and may have made significant contributions to the tetracycline binding in the Fe–BC composite compared to pristine BC (Yang X. et al., 2016). Zhou et al. (2017) achieved similar results regarding tetracycline sorption using Zn–Fe sawdust BC composite. The Zn–Fe–BC composite showed the highest sorption amount compared to unmodified BC. Furthermore, the material manufactured by subjecting the feedstock to the action of a mixture of both Zn–Fe showed a fourfold enhancement in the q_{max} amount compared to the original BC (Zhou et al., 2017). Chen et al. (2019) examined the sorption capacity of Fe_2O_3–BC composite for levofloxacin and tetracycline. The creation of the BC composites involved soaking the biomass with Fe_2O_3 pre-treatment (before pyrolysis) and post-treatment (after pyrolysis). The post-treated Fe–BC composite was exposed to comprise hydrated amorphous iron (III) oxide, whereas crystalline γ-ferric oxide was prevalent in the pre-treated Fe–BC composite (Chen et al., 2019). It was observed that the post-treated Fe-BC composite, although it has lower iron content and surface area, exhibited a much higher amount of q_{max} for antibiotics observed (by 400% for levofloxacin and 50% for tetracycline) than pre-treated Fe–BC composite. This is attributed to the presence of many hydroxyl moieties in the post-treated Fe–BC composite, contributing to the sorption. The sorption mechanism exposed that F-replacement with hydroxyl groups (-OH) contributed to the antibiotic binding with the prepared composites, H-bonding, electrostatic attraction, and complexation (Chen et al., 2019). In addition, both composites' regeneration abilities after five adsorption–desorption cycles were examined. The decrease in adsorption for both modified BCs did not surpass 20% compared with the freshly obtained BCs, which exhibited their practical effectiveness (Chen et al., 2019). Li et al. (2018) investigated the Fe/Mn–BC composite removal capacity for enrofloxacin, ciprofloxacin, and norfloxacin. The prepared composite was characterized by 2 times higher pore volume and 1.5 times higher surface area than the pristine BC. Compared with the unmodified BC, the composite showed a higher sorption amount of 20%–63% for the selected three antibiotics examined. The sorption is enhanced in the following order: norfloxacin < ciprofloxacin < enrofloxacin.

The noticed variations in the effect of treatment on the antibiotic sorption were owing to the little different properties and structures of the antibiotics molecules. It could be attributed to the introduction of more O-enriched functional groups on the composite surface and higher porosity increased sorption onto the modified BC relative to the unmodified BC (Li et al., 2018). The sorption of targeted antibiotics is enhanced with decreasing ionic strength and pH of the solution. It was confirmed that after three adsorption–desorption cycles, the Fe/Mn–BC composite maintained about 100% of the original adsorption amount toward the examined enrofloxacin, ciprofloxacin, and norfloxacin (Tan et al., 2016a). Tan et al. (2016b) prepared an Mg/Al–BC composite that was employed to examine tetracycline adsorption. The results showed that the highest amount of tetracycline was adsorbed onto the modified BC compared to the untreated BC. This was attributed to the presence of various alkoxide and hydroxide groups in the modified-adsorbent structure, contributing to H-bonding with the tetracycline molecule (Tan et al., 2016a). Furthermore, π–π and electrostatic interactions were proposed among the mechanisms accountable for tetracycline binding to the Mg/Al–BC composite (Tan et al., 2016b). Heo et al. (2019) synthesized a magnetic BC with zinc ferrite for sulfamethoxazole removal. The modified BC was characterized by about 60% greater sulfamethoxazole sorption amount compared with the unmodified BC. This was attributed to the higher pore volume, surface area, and porosity of the composite than those of the unmodified BC (Heo et al., 2019). Moreover, enhancement in sulfamethoxazole adsorption capacity onto the modified BC was associated with sorption mechanisms (i.e., π–π EDA interactions). It was exposed that the Me-O groups participated in antibiotic binding by complexation and H-bonding. The regeneration and usefulness ability of the prepared BC composite were also examined. After four consecutive cycles, the composite still exhibited a 90% sulfamethoxazole adsorption efficiency compared with its worth for pristine adsorbent (Heo et al., 2019). Sun et al. (2022) reported that the $FeCl_3$–BC composite showed higher adsorption capacities for sulfamethoxazole, sulfamethazine, and sulfadiazine as 454, 400, and 294 mg g^{-1}, respectively, compared to the unmodified adsorbent. This could be attributed to the higher surface area of composite, H-bonding between -COOH/-OH groups in adsorbent and antibiotics molecules. The sorption amount at low pH was comparatively high due to the hydrophobic interactions, van der Waals forces, pore-filling, electrostatic attraction, charge-assisted H-bonding, and the combination of π–π EDA. The findings of this study exhibit that $FeCl_3$-modified adsorbent has potential applications as an efficient, recyclable composite for antibiotic elimination from wastewater (Sun et al., 2022). Liang et al. (2022) found a higher sorption capacity (38.70 mg g^{-1}) of $CaCl_2$/$FeCl_2$-modified BC for norfloxacin than pristine BC. Furthermore, the adsorption mechanism of norfloxacin on composite was thermodynamically spontaneous (Liang et al., 2022). In brief, the application of engineered/modified BCs is aimed at increasing the removal efficiency of antibiotic residues from aqueous. This is rigorously dependent on the physicochemical characteristics of both the adsorbate and adsorbent as well as sorption conditions. In the case of BC composites, the presence of more components may alter the characteristics, influencing the mechanisms and process of antibiotic removal and adsorption. Depending on the kinds of clay minerals, their loading to the BC matrix can improve porosity, alter surface charges, and provide cations or oxygen polar functional groups. Therefore, in addition to the typical sorption mechanisms for BC, the contribution of interactions, including pore-filling or polar groups, can be enhanced. Moreover, ion exchange and drug intercalation between the clay layers can occur. Mixing BC with carbon nanomaterials usually enhances the porosity properties, in the case of graphene loading, and the formation of O-enriched functional groups. In contrast, among the mechanisms accountable for the adsorption of the antibiotic on this type of BC composites, the paramount contributors may be interactions with O-containing groups, pore-filling, π–π interactions, and hydrophobic resultant from the structure carbon materials. Metal components in metal–BC composites are accountable for altering the surface charge and provide oxygen-enriched functional groups. The metal complexation, H-bonding, and electrostatic interaction can also be distinguished.

Sorption of organic pollutants and dyes with biochar-based engineered composites

The major organic pollutants in an aqueous medium are pharmaceuticals, pesticides, and PAHs. For the adsorption of organic contaminants, the modified BC has been widely used. Modified BCs have been extensively used for the adsorption of organic pollutants (Murtaza et al., 2021b). The removal efficiency of phenanthrene was enhanced by 63% to 94% with an increase in the graphene ratio of BC in the range of 0%–1%. The adsorption mechanism occurred by partitioning, pore-filling, electrostatic attractions, surface adsorption, and π–π EDA interaction (Gai et al., 2014). Graphene coating on the BC surface resulted in higher pore volume, pore size, surface area, a large number of oxygen-enriched functional groups, enhancement of negative surface charge, and strong vibration of the C=C bonds. Thus, graphene-coated BCs more effectively eliminate phenanthrene than unmodified BC (Table 5). Pristine BC derived from bagasse, rice husk, and wheat straw showed very low methylene blue removal capacity. After the modification of these BCs with clay minerals (montmorillonite and kaolinite), the sorption efficiency increased. Nonetheless, these modifications slightly decreased the methylene blue removal by the BC composite with montmorillonite and kaolinite, possibly owing to the blockage of pores with clay

particles (Yao et al., 2014) (Table 5). ZnVI and chitosan-coated BCs achieved greater removal of methylene blue from wastewater than untreated BC. Among all the Fe-modified BCs, the BC composite with a higher quantity of Fe reached the highest methylene blue removal capacity. This increased sorption can be due to chemical reduction and surface adsorption mechanisms (Miyajima and Noubactep, 2012). The removal efficiency of molybdenum by ZnVI-treated BC derived from rice husk was observed in composite synthesized with different ratios (ZnVI: BC, 1:3, 1:5, and 1:7). The highest molybdenum sorption efficiency for prepared composites was exposed at a ratio of 1: 5 (98%) and more rise of ratio to 1:7 slightly reduced the molybdenum removal capacity (around 95%) (Han et al., 2015). Activated and magnetic BCs were produced using husk and tannin BC. The removal capacities of magnetic and activated BCs for thiamethoxam and thiacloprid were 0.73 and 1.02 mg g^{-1}, respectively. Pesticide adsorption onto activated BC occurred by π–π interactions owing to the available aromatic rings in BC, whereas the magnetic BC had a large amount of –OH (polar groups) (Han et al., 2015). Zhao et al. (2013) prepared a Fe_3O_4–BC composite to observe the removal of polybrominated diphenyl ethers (PBDEs) from contaminated water. The results exhibited that the modified BC was more efficient for the PBDEs removal than other pristine BCs (Zhou et al., 2013). Zhang M. et al. (2014) presented that the MgO-doped BC removal capacity for DFY anionic dye was significantly higher than unmodified BC. It was determined that the surface of BC may be positive after MgO doping, due to the presence of a large amount of functional groups, which increased the DFY sorption (Zhang X. N. et al., 2014). Inyang et al. (2014) studied the methylene blue removal efficiency of unmodified bagasse and hickory adsorbents and CNT-modified composite (CNT–hickory BC and CNT–bagasse BC). The highest removal capacities of CNT–bagasse BC composite and CNT–hickory BC composite (5.5 and 2.4 mg g^{-1}, respectively) were higher than those of their pristine BCs (2.2 and 1.3 2.4 mg g^{-1}, respectively). The dominant mechanism was an electrostatic attraction for the methylene blue sorption and strong affinity binding sites within CNT (Jing et al., 2014). Nonetheless, the CNT–BC composite preparation procedure is inexpensive and very simple, and the CNT–BC composite can be used as a promising adsorbent for the removal of organic contaminants and dyes from the water system (Rajapaksha et al., 2016). Ghaffar and Younis (2014) observed the methylene blue and phenol sorption by the graphene-loaded BC. Higher pore volume and surface area after graphene doping on the adsorbent may be the major reason for sorption enhancement. Moreover, π–π bonding between methylene or phenol molecules and graphene sheets contributed to improving the sorption capacity (Ghaffar and Younis, 2014). Zhang et al. (2012) noticed a significant enhancement of methylene blue sorption on graphene-loaded BC composite, and stronger π–π bonding between methylene blue and graphene sheets on the adsorbent surface was conceived to be the dominant mechanism for the increase in methylene blue sorption *via* the graphene-loaded adsorbent (Zhang et al., 2013). Li et al. (2019) prepared a BC composite with Mn–Fe oxides and observed its removal capacity for naphthalene from contaminated water. The composite showed higher removal capacity compared to the unmodified adsorbent, possibly due to the generation of oxygen species with the aid of Mn(II) and Fe(III) coupling (Li et al., 2019).

Sorption of inorganic pollutants with biochar-based engineered composites

Modification to create BC-based composites uses the BC as a scaffold to embed new materials to form surfaces with novel surface attributes upon which inorganic contaminants can sorb. Sorption of the inorganic contaminants through engineered BC results from surface precipitation, electrostatic attraction, and stoichiometric ionic exchange. In this section, we demonstrate how the engineered BC composite increases the elimination of inorganic pollutants from wastewater.

Sorption of heavy metals through biochar-based engineered composites

The most commonly found heavy metals in the water system are Cu, Zn, Cd, As, Cr, Hg, and Pb. The EPA has set permissible limits for the metals in wastewater and drinking water. Thus, different methods were used, such as reverse osmosis, chemical precipitation, ion exchange, electro-dialysis, adsorption, and solvent extraction, to eliminate trace metals from polluted water. Due to relative expensiveness, adsorption is considered an economically feasible technique for eliminating heavy metals from the water system (Table 5). The removal efficiencies of bentonite-loaded BC for Zn (II) and Cr (VI) were lower as compared to raw bentonite and pristine BC, and it was proposed that the binding of anionic functional groups of BC with the cationic compounds of bentonite may have decreased the present sorption sites (Fosso-Kankeu et al., 2015). Wang M. C. et al. (2015) produced a hematite-loaded BC derived from pinewood, resulting in an arsenic removal capacity nearly double that of untreated BC. Zhou et al. (2017) prepared a BC composite with magnetized gelatin. This composite showed three-time enhancement in maximum sorption of As^{5+} from wastewater, ascribed to the higher electrostatic attraction of As^{5+} to Fe_2O_3 particles and protonated O-enriched functional groups available on the surface of BC (Zhou et al., 2017). The sorption of As^{5+} onto hematite-loaded BC was almost double that of the unmodified BC, further proposing that Fe_2O_3-particles contribute as sorption sites with a strong affinity than pristine BC for As^{5+} in the aqueous medium (Komnitsas et al., 2015).

TABLE 5 Adsorption capacity of engineered biochar campsites to eliminate pollutants in contaminated water (heavy metals, nutrients, and organic contaminants).

Biochar	Modifying agent	Pyrolysis temperature (°C)	Pyrolysis time	Pollutant	Enhancement in adsorption	Involved mechanism	Reference
Rice husk	Fe	300	1 h	Cr^{6+}	Elimination percentage of Cr^{6+} was marginally enhanced after using the engineered composite	Electrostatic interaction, repel negatively charged Cr^{6+}	Agrafioti et al. (2014)
Rice husk	Ca^{2+}	300	1 h	As^{5+}	Removal efficiency of As^{5+} enhanced by 70% compared to pristine biochar	Owing to alkaline solution of calcium oxide eliminate As^{5+} by precipitation	Agrafioti et al. (2014)
Solid waste	Ca^{2+}	300	1 h	Cr^{6+}	Removal percentage of Cr^{6+} significantly enhanced with modified biochar	Repulsion negatively charged Cr^{6+} and higher pH of engineered biochar deprotonate their functional groups	Agrafioti et al. (2014)
Solid waste	Fe	300	1 h	As^{5+}	Removal capacity of As^{5+} expressively using Fe-modified biochar	As^{5+} eliminate *via* co-precipitation	Agrafioti et al. (2014)
Pinewood	Hematite	600	1 h	As^{5+}	The Υ-Fe_2O_3 particles serve as sorption sites for As^{5+} and enhance the removal efficiency of As^{5+}	The electrostatic interactions observed a leading mechanism in adsorption. Modified biochar has shown magnetic characteristics owing to the conversion of hematite into Υ-Fe_2O_3 particles with magnetic traits	Wang S. et al. (2015)
Bamboo	ZnV iron	600	1 h	Methylene blue	Modified biochar showed the maximum removal capacity against methylene blue	—	Zhou et al. (2014)
Bamboo	Montmorillonite	400	1 h	Phosphate	Removal efficiency for P is 8 times greater than pristine biochar	Phosphate adsorption was accelerated by electrostatic attraction	Chen et al. (2017)
Bamboo	ZnV iron	600	1 h	Pb^{2+}	About 90% of Pb^{2+} was eliminated	Electrostatic attraction among ZnV iron particles and anions on the engineered biochar surface	Zhou et al. (2014)
Bamboo	Montmorillonite	400	1 h	Ammonium	Observed higher adsorption capacity	Mechanism occurred by surface adsorption onto modified biochar	Chen et al. (2017)
Bamboo	ZnV iron	600	1 h	Phosphate	Removal enhanced by 55%	Co-precipitation	Zhou et al. (2014)
Sorghum bagasse	Bentonite	400	4 h	Zn^{2+}	Removal efficiency of modified adsorbent was lower for Zn^{2+} than pristine biochar and bentonite	Anionic functional groups on the BC that partially bind with the cationic compounds in bentonite and block pores	Fosso-Kankeu et al. (2015)
Bamboo	ZnV iron	600	1 h	As^{5+}	Adsorption capacity of As^{5+} by ZnV iron-modified biochar enhanced by 70%	Electrostatic attraction	Zhou et al. (2014)
Hickory chip and bamboo bagasse	Montmorillonite	600	1 h	Methylene blue	Removal capacity of methylene blue with both engineered biochars has been increased compared to unmodified biochars	Higher ion exchange capability of montmorillonite clay enhanced the adsorption rate of modified biochar	Yao et al. (2014)
Sorghum bagasse	Bentonite	400	4 h	Cr^{6+}	Removal rate of Cr^{6+} by bentonite-modified biochar	Surface adsorption onto modified biochar	Fosso-Kankeu et al. (2015)

(Continued on following page)

TABLE 5 (*Continued*) Adsorption capacity of engineered biochar campsites to eliminate pollutants in contaminated water (heavy metals, nutrients, and organic contaminants).

Biochar	Modifying agent	Pyrolysis temperature (°C)	Pyrolysis time	Pollutant	Enhancement in adsorption	Involved mechanism	Reference
					is greater than pristine biochar and bentonite		
Bamboo	ZnV iron	600	1 h	Cr^{6+}	Elimination of Cr^{6+} enhanced with the addition of ZnV iron-modified biochar	Electrostatic attraction among ZnV iron particles and anions on the engineered biochar surface	Zhou et al. (2014)
Hickory chip and bamboo bagasse	Kaolinite	600	1 h	Methylene blue	Removal capacity of methylene blue by modified biochars slightly enhanced compared to raw biochar	—	Yao et al. (2014)
Sorghum bagasse	Bentonite	400	4 h	Malachite green	Adsorption capacity of malachite green was greater compared to raw biochar	Negative charge of modified biochar enhanced the attraction of cationic dyes through electrostatic interactions	Fosso-Kankeu et al., (2016)
Gumwood	Carbon nanotube and graphene oxide	600	1 h	Cd^{2+}, Pb^{2+}	Removal capacities for Cd^{2+} and Pb^{2+} were greater compared to raw biochar. Graphene oxide-modified biochar exhibited greater removal of Cd^{2} and Pb^{2+} compared to carbon nanotube-modified adsorbent	Co-precipitation	Liu et al. (2016)
Bamboo	Chitosan	600	1 h	Pb^{2+}	Elimination of Pb^{2+} higher than 35% compared to unmodified biochar	Amine functional groups of chitosan have a resilient association with cationic metal ions in aqueous	Zhou et al. (2014)
Wheat straw	Graphene	600	1 h	Mercury, phenanthrene	Removal capacity of mercury and phenanthrene improved with the enhancement in graphene amount	Engineered biochar surface showed more O-enriched functional groups, which enhanced the removal of mercury and phenanthrene	Tang et al. (2015)
Bamboo	Chitosan	600	1 h	Cr^{6+}	Removal of Cr^{6+} increased from 27% compared to pristine biochar	Co-precipitation	Zhou et al. (2014)
Pinewood	MgO	600	1 h	Nitrate and phosphate	Removal rate of nitrate was 5%, and removal rate of phosphate was 0.5%	Electrostatic repulsion	Zhang et al. (2012)
Bamboo	Chitosan	600	1 h	Methylene blue	Adsorption efficiency was high	Surface of chitosan-modified and pristine biochar negatively charged	Zhou et al. (2014)
Peanut shell	MgO	600	1 h	Nitrate and phosphate	Adsorption efficiency was high for both pollutants	Complexation mechanism	Zhang et al. (2012)
Sugar beet	MgO	600	1 h	Nitrate and phosphate	Adsorption rate of phosphate was 66%, and nitrate adsorption rate was 11%	MgO has a strong attraction for P in aqueous owing to its high affinity for anions *via* mono-nuclear, bi-	Zhang et al. (2012)

(Continued on following page)

TABLE 5 (*Continued*) Adsorption capacity of engineered biochar campsites to eliminate pollutants in contaminated water (heavy metals, nutrients, and organic contaminants).

Biochar	Modifying agent	Pyrolysis temperature (°C)	Pyrolysis time	Pollutant	Enhancement in adsorption	Involved mechanism	Reference
						nuclear, and tri-nuclear complexation	
Corncob	$Fe(NO_3)_3$	500 and 700	2 and 3 h	As	Engineered biochar shows about 20-time enhancement of removal for As compared to pristine biochar	Co-precipitation	Fristak et al. (2017)
Bamboo	Chitosan	600	1 h	As^{5+}	Did not eliminate anionic As^{5+} from the solution	—	Zhou et al. (2014)
Corncob	Mn	500 and 700	1 h	Pb^{2+}	Biochar soaked with 3% Mn showed the maximum Pb^{2+} removal percentage (99%)	Large amount of the hydroxyl group accelerated the Pb^{2+} removal	Wang M. C. et al. (2015)
Switchgrass	Magnetic composite	425	2 h	Metribuzin (herbicide)	Adsorption capacity was 39.6 mg g^{-1}, greater than fresh biochar	Hydrogen-bonding and electrostatic interaction	Essandoh et al. (2017)
Rice husk	Fe(III)	300	1 h	Cr^{6+}	Removal percentage of Cr^{6+} by Fe(III)-modified biochar enhanced with the reduction of Fe(III) quantity in modified material	Strongly acidic conditions cause an influence on the solubility of Fe(III), which negatively affects Cr^{6+} adsorption on biochar	Agrafioti et al. (2014)
Rice husk	Fe(III)	300	1 h	As^{5+}	Removal rate of As^{5+} through Fe(III)-modified biochar enhanced by about 47% compared to pristine biochar	Greatly acidic nature of the solution stimulates electrostatic interactions between negatively charged As^{5+} species and positively charged biochar surface	Agrafioti et al. (2014)
Bio solid	Fe	500	4 h	As(V)	Removal capacity archived at 67.2 mg/g was higher compared to pristine biochar	Owing to the strong affinity of arsenate active sites and endothermic mechanism	Rahman et al. (2022)
Bio solid	Zr-Fe	300	30 min	As(V)	Zr–Fe-modified biochar achieved 62 mg/g, more higher than raw biochar	Adsorption process was endothermic and spontaneous, formation of the inner sphere, and electrostatic attraction	Rahman et al. (2020)
Coffee husk and corncob	ZnO	600	2 h	As(V), Pb^{2+}	Removal capacity of As(V) is 25.9 mg/g and that of Pb^{2+} is 25.8 mg/g, respectively	Improving the microstructure of modified biochars increased the active sites, electrostatic attraction	Cruz et al. (2020)
Rice straw	$FeCl_3$	450	1 h	As(V)	Compared to pristine biochar, Fe-loaded biochar exhibited a much higher capacity to eliminate As(V) from wastewater	Resilient electrostatic attraction between surface functional groups and anions species in solution that could boost the adsorption mechanism	Nham et al. (2019)
Rape straw	Ferrihydrite	400	2 h	Cd(II)	Higher adsorption capacity observed at 18.18 mg g^{-1} compared to pristine biochar was five times higher	Complexation, ion exchange, and electrostatic interaction	Tian et al. (2022)
Date palm leaves	$Fe(NO_3)_3$	300, 500, and 800	4 h	As	$Fe(NO_3)_3$-treated composite achieved a great removal capacity of up to 97%	Enhancing sorption sites because of higher changes in biochar characteristics	Kirmizakis et al. (2022)
Bamboo	CO-Fe	500	2 h	Cr^{6+}	Maximum adsorption (51.7 mg/g) capacity observed, five times higher than untreated biochar	CO–Fe-binary oxide was uniformly generated, and higher surface area after loading Co-Fe on	Wang et al. (2013)

(Continued on following page)

TABLE 5 (*Continued*) Adsorption capacity of engineered biochar campsites to eliminate pollutants in contaminated water (heavy metals, nutrients, and organic contaminants).

Biochar	Modifying agent	Pyrolysis temperature (°C)	Pyrolysis time	Pollutant	Enhancement in adsorption	Involved mechanism	Reference
						biochar, strong electrostatic attraction	
Poplar	$FeCl_3$	300 and 600	2 h	As^{3+} and As^{5+}	Increased the adsorption from 86.8% to 99.9% for As^{5+} and from 73.8% to 99.9% for As^{3+}	Spatial distribution and species of arsenic, introduction of calcite on the composite surface	Xu et al. (2020)
Populus wood	$FeSO_4$	300 and 600	2 h	Hg^{2+} and Cr^{6+}	Fe-treatment boosted the removal capacity from Hg^{2+} (62.5%) and Cr^{6+} (97.0%)	Redox reaction accelerated the elimination process	Feng et al. (2019)
Wheat straw	$Fe(NO_3)_3$	650	3 h	Se(VI)	Modification greatly improved biochar's capacity for Se(VI) removal, and adsorption capacity was noticed (14.3 mg g^{-1})	Creation of Se complexes with the Fe compounds existing on the surface of biochar	Godlewska et al. (2020)
Macroalgal biomass	$FeCl_3$	300, 450, and 750	1 h	Molybdenum, arsenic, and selenium	Fe-modified biochar showed higher sorption capacity for molybdenum (64%–78%), arsenic (62%–60%), and selenium (14%–38%) was higher than raw biochar	High affinity for oxyanions and electrostatic interaction	Johansson et al. (2016)
Food waste	$Fe(NO_3)_3$	300, 450, and 600	4 h	Se(VI)	Attain the maximum selenium removal, applying modified biochar	Endothermic adsorption mechanism	Hong et al. (2020)
Peanut shell	$Fe_2H_2O_4$	600	1 h	Cu^{2+}, Cd^{2+}	Excellent performance for adsorption of Cu^{2+} and Cd^{2+} for 34.1 ^{1}and 29.9 mg g^{-1}, respectively	Complexation and surface adsorption	Li et al., (2020)
Rice husk	S	550	2 h	Hg^{2+}	Removal capacity was 73%, higher than other used unmodified biochars	Surface deposition and pore-filling	O'Connor et al. (2018)
Peanut shell	Hydrated MnO	400	1 h	Pb^{2+}	Higher sorption capacity compared to raw biochar	Complexation, ion exchange, and electrostatic interaction	Wan et al. (2018)
Cottonwood	Layered double hydroxides	180	2 h	PO_4^{3+}	Achieved the adsorption (386 mg g^{-1}), greater than other unmodified biochars	Surface adsorption	Zhang M. et al. (2014)
Tomato leaves	Mg-loaded	600	2 h	PO_4^{3+}	Adsorption capacity was 100 mg g^{-1} higher than unmodified biochar	Surface deposition and precipitation	Yao et al. (2013)
Cottonwood	$AlCl_3$	600	2 h	PO_4^{3+}	Adsorption capacity achieved 835 mg g^{-1}	Surface adsorption	Zhang and Gao (2013)
Wood waste	MgO	600	2 h	PO_4^{3+}	Adsorption capacity archived 116.4 mg g^{-1}	Surface adsorption and precipitation	Xu et al. (2018)
Bamboo	Mg/Al	600	2 h	PO_4^{3+}	Adsorption capacity archived 13.11 mg g^{-1}	Surface adsorption and anion exchange	Wan et al. (2017)
Hickory wood	Aluminum salt	600	2 h	Phosphorus	Sorption capacity achieved 8.346 mg g^{-1}	Electrostatic attraction	Zheng et al. (2019)
Peanut shells	$MgCl_2$	600	2 h	NO_3^-	Sorption capacity achieved 94 mg g^{-1}	Surface adsorption	Zhang et al. (2012)
Wheat straw	Mg/Fe	600	2 h	NO_3^-	Adsorption capacity archived 24.8 mg g^{-1}	Anion exchange and surface adsorption	Xu et al. (2019)
Wood waste	MgO-treated	600	2 h	NH_4^+	Adsorption capacity archived 47.5 mg g^{-1}	Surface precipitation	Xu et al. (2018)

Wang S. et al. (2015) observed that MnO_2-modified BC showed significantly increased adsorption capacity for Pb and As (Wang M. C. et al., 2015). Among three BC composites produced by mixing with different manganese ratios, the maximum adsorption capacity for Pb^{2+} (about 98%) was revealed *via* BC composite doped with 3.65% manganese. Nonetheless, the BC composite doped with a very high amount of manganese showed low Pb^{2+} adsorption capacity because doping decreased the surface area by pore blockage (Wang S. et al., 2015). The pH of the solution influenced the composite surface net surface charges and Pb^{2+} species, which directly influenced the Pb^{2+} sorption (Wang M. C. et al., 2015). Hg removal improved with an increase in the graphene amount from 0.1% to 1% in a wheat straw–graphene BC composite (Tang et al., 2015). The mercury removal was accelerated by the higher surface area, granting surface complexation between mercury and improved O-enriched functional groups on the composite surface comprising 1% graphene (Li et al., 2015). Shang et al. (2016) observed that the Cr^{6+} removal capacity from contaminated water by graphene oxide-modified BC derived from hyacinth was significantly higher compared to the untreated BC. They suggested that Cr^{6+} sorption onto modified BC was likely through the electrostatic attraction of Cr^{6+} coupled with Cr^{6+} reduction to Cr^{3+} and Cr^{3+} complexation. With the enhancement of the sorption capacity of Pb^{2+} with the CNT-doped BC, Pb^{2+} was likely adsorbed *via* electrostatic attraction with O-enriched groups in carbon nanotubes loaded BC surface (Inyang et al., 2015). Chitosan-treated BC increased the Pb^{2+} removal more than that of the untreated BC because the chitosan amine functional groups had higher affinities to cationic metal ions in the water system (Zhou et al., 2013). The treatment with chitosan and ZnVI increases the Pb^{2+} removal up to 90%, which is exempted from the ZnVI amount present in the modified BC. Nonetheless, Cr^{6+} removal enhanced with an increasing quantity of ZVI in the modified BC; the maximum removal rates noticed were 30% and 35%, signifying that both ZnVI particles and chitosan conferred improvement to the elimination of cationic trace metals (Zhou et al., 2014). Chitosan-treated and unmodified BCs did not attain noteworthy As^{5+} removal from aqueous solution, possibly because their surfaces had negative charges (Zhou et al., 2013). Nevertheless, the ZnVI-modified BC sorbed between 20% and 90% of As^{5+}, and raising the Fe-level in modified BC enhanced the removal of As^{5+} (Almeelbi and Bezbaruah, 2012). Fe- and Ca-modified BCs showed great As^{5+} removal efficiencies (up to 90%) compared to pristine rice husk BC, which removed 50%. Nonetheless, the removal rate of As^{5+} was not as great as estimated; the maximum removal capacity (up to 90%) was attained by Fe^{3+}-modified BC derived from rice husk (Agrafioti et al., 2014). Sweet gum-derived BC modified with CNT and graphene achieved greater sorption capacities for Cd^{2+} and Pb^{2+} than unmodified BC. The graphene-BC composite showed higher sorption of Cd^{2+} and Pb^{2+} than the CNT-BC composite. Sorption of Cd^{2+} and Pb^{2+} could be regulated by complexation with O-enriched functionalities of the CNT materials, cation exchange, surface adsorption, and electrostatic attractions onto the BC, graphene, and CNT composite surface (Inyang et al., 2014). Fe_2O_4-impregnated BC showed low removal capacity for Cd^{2+} and Pb^{2+}, elimination was obviously pH-dependent, and sorption capacity was enhanced with an increase in pH from 2 to 8. At acidic pH, due to the presence of a higher amount of H^+ on the modified BC composite, the surface of BC was protonated and became positively charged (Agrafioti et al., 2014). The Cu^{2+} sorption capability of MnO_2-treated BC increased with the increase in pH between 3 and 6 and was relatively greater than the unmodified adsorbent. Generation of the complexes between Cu^{2+} and O-enriched functional groups available on the surface of the composite was the main mechanism involved in the metal sorption (Zhou et al., 2017). Magnetic BCs produced by impregnating with various mass ratios of $NaBH_4$ and $FeSO_4$ exhibited a strong affinity for Cu^{2+}, and the sorption affinity enhanced with the increase in $NaBH_4$ and $FeSO_4$ molar ratio in modified BCs. The sorption amount was enhanced with the long stirring time and reduced with the higher initial concentration of Cu^{2+} in the aqueous solution. The leading functional groups bestowing to the coordination of the Cu^{2+} on the BC surface were hydroxyl, phenolic, and carboxyl groups. Partial deprotonation of the functional groups under acidic conditions stimulated the Cu^{2+} sorption by exchanging Cu^{2+} with H^+ (Kolodynska and Bak, 2017). A higher removal capacity of Pb^{2+} was exhibited *via* ZnS-modified BC compared to raw BC. Nonetheless, it was pH-dependent, and up to pH 6, Pb^{2+} precipitated as hydroxide. The sorption of Pb^{2+} was proposed as a spontaneous and endothermic mechanism (Ling et al., 2017). Li et al. reported that $Fe_2H_2O_4$-modified peanut shell showed excellent performance for the adsorption of Cu^{2+} and Cd^{2+} for 34.1 and 29.9 mg g^{-1}, respectively. The modified BC exhibited adequate anti-interference capability for Cu^{2+} and Cd^{2} elimination in the presence of great levels of Mg^{2+} and Ca^{2+} due to specific inner-sphere complexation between immobilized modified composite and Cu^{2+} and Cd^{2+}. Wan et al. (2018) loaded hydrated MnO into a peanut shell-produced BC, showing excellent removal performance for Pb^{2+} compared to other used raw BCs (Wan et al., 2018). The removal capacity of $MgCl_2$–BC composite to Cd^{2+} was 763 mg g^{-1}, which was 11 times higher than that of raw BC. The Cd^{2+} removal *via* BC composite was primarily due to the following process: Cd $(OH)_2$ precipitation (73%) > ion exchange (22%) > Cd^{2+}–π interaction (3.88%), with slight interactions from functional group complexation, physical adsorption, and electrostatic attraction (Yin et al., 2021). Van Vinh et al. (2015) stated that the sorption capacity of arsenic (III) is increased from 5 to 7 μg/g by Zn $(NO_3)_2$-loaded BC. In conclusion, BC-based composite could efficiently remove the heavy metals, and the sorption capacity was greatly affected by ions, solution pH, water quality, and temperature. The leading adsorption mechanisms

of heavy metal ions were surface complexation, ion exchange, and precipitation.

Immobilization of heavy metals by compositing and anaerobic digestion of biomass

Compositing and anaerobic digestion are important methods potentially used to immobilize heavy metals. The eco-toxicity and bioavailability of heavy metals rely upon their chemical composition, which could be altered through compositing and anaerobic digestion (Zhu et al., 2014). Based on the European Community Bureau of Reference, heavy metals can be divided into four chemical fractions: exchangeable fraction/acid soluble (fraction 1, F1), reducible (fraction 2, F2), oxidizable (fraction 3, F3), and residual (fraction 4, F4) (Zheng et al., 2021). Studying the chemical fractions and immobilization of heavy metals is of utmost importance for exploring their toxic impacts on the environment (Zheng et al., 2022). It has been found that compost and biogas residue contained a high content of heavy metals due to the degradation of organic matter (Wainaina et al., 2020). Most heavy metals in biogas residue and compost exhibited a higher range than relevant standards. In anaerobic digestion, the reduction of inorganic phosphorus increased the bioavailable fraction proportion in Cd and Zn but decreased the F4 proportion and manifested moderate environmental risks (Yan et al., 2018; Cui et al., 2021). In the digester, arsenic (As (III) was the dominant species that induced a substantial increase in As toxicity (Pous et al., 2015). In contrast, the F3 proportion in copper (Cu) and Pb in biogas residue were increased mainly due to the sulfide formation (Zhang et al., 2016). However, compost carried a high proportion of humus, which increased the proportion of F3 in Cu but reduced the F1 proportion in Zn (Legros et al., 2017; Le Bars et al., 2018). However, plant availability of Zn did not decrease in compost. During composting, Cd and As convert bioavailable fractions into stable fractions, and As (V) toxicity becomes a major concern (Zheng et al., 2022). Therefore, to improve the treatment of manure and make its use safer, combining more comprehensive methods with low economic costs is necessary.

Sorption of nutrients through biochar-based engineered composites

The release of nutrients, for instance, phosphate, ammonia, and nitrate, to the natural environment enhances the amount of growth-limiting nutrients in the natural water system and stimulates the growth of photosynthetic pigments, which can eventually lead to eutrophication of the aquatic environment. Though phosphate can be sorbed by several adsorbents, the parallel mechanism for nitrate is slightly difficult. Nonetheless, BC can eliminate phosphate, ammonia, and nitrate from an aqueous solution (Yao et al., 2013). Generally, BC is impotent in eliminating nitrates, and a few BCs release phosphate and nitrate into the solution (Gai et al., 2014). At high pH, the sorption capacity of phosphate is reduced because of the negatively charged BC surfaces (Gai et al., 2014). However, compared to pristine BCs, engineered BCs have shown great potential in eliminating nutrients from aqueous medium. Table 5 summarizes the modified BC application in the sorption of pollutants available in the water system. For instance, BC modification can induce differential sorption effects for the same pollutant, possibly due to the effect of feedstocks (Zhang et al., 2012). The unmodified BC has exposed an extremely low removal rate of around 10%, compared to MgO-modified BC derived from wheat straw (66%), which is explicated by the high affinity of MgO for phosphate in aqueous solution due to its high affinity for anions by mono-, bi-, and tri-nuclear complexation (Yao et al., 2013). Nevertheless, the complexation process depends on the distribution and amount of MgO particles on the surface of BC. Interestingly, MgO-modified BC derived from peanut shells achieved a lower removal rate of phosphate at 0.5% (Zhang et al., 2012). The electrostatic repulsions between the phosphate and BC surface in solution were the main reason for the low sorption of phosphate *via* MgO-modified BC derived from peanut shells (Lou et al., 2016). The removal of nitrate by MgO-modified BC derived from wheat straw and MgO-modified BC derived from peanut shell was observed to be 3.6% and 11.7%, respectively, which might be due to differences in the sorption processes involved (Zhang et al., 2012). Chitosan-treated BC had not reached promising consequences in the phosphate removal from the solution due to the net negative charge of the treated BC surface (Zhou et al., 2014). In contrast, ZnVI-treated BC sorbed a high amount of phosphate, and elimination capacity was observed to improve from 50% with enhancing the amount of iron. The pH of the solution (5.7) was lower than the pH_{pzc} (7.7) of ZVI. Therefore, the cationic form mainly present in this solution might have stimulated the binding of phosphate (Almeelbi and Bezbaruah, 2012). The increased adsorption capacities shown by the montmorillonite-modified BC for phosphate and ammonium were due to the increased surface area of BC and increased amount of binding sites led by clay doping (Almeelbi and Bezbaruah, 2012). The sorption of ammonium and phosphate on the montmorillonite-modified BC at low amounts was mostly controlled by chemical adsorption. However, at greater concentrations, the physical and chemical adsorption mechanisms involved through multilayer sorption also played a vital role (Chen et al., 2017).

Factors affecting pollutant adsorption

Effect of solution pH and reaction temperature

Solution pH is considered the most important parameter of metal sorption (Qin et al., 2011). It has been described that the solution pH affects the adsorption of pollutants onto engineered/modified BCs. This is associated with the O-enriched functional groups, which are pH-dependent. Thus, the ionization and surface charge at the BC surface are pH-dependent, contributing to differentiating sorption capacity to eliminate pollutants (Zhang et al., 2013). Lu et al. (2012) reported that the deprotonation of the functional groups occurs when the solution pH increases. This contributes to enhancing the adsorption rate of the adsorbents toward cationic metals. Nonetheless, if the solution pH reduces, it contributes to enhancing the electrostatic repulsion forces between the metal ions and protons in the solution. Therefore, competition between cations for the sorption sites of the adsorbent can happen, resulting in reducing the amount of adsorbent material for the metal ions. In their study to remove the metals such as lead, zinc, and copper using BC-based composite created from corn straw and hardwood, Chen et al. (2011) presented that enhancement in the solution pH from 2 to 5 contributes to improvement in the sorption rate of metallic cations. More than 5 pH lessened the sorption amount due to hydroxide complex formation. The same results were presented by Lu et al. (2012). Nonetheless, Zhang et al. (2013) suggested that reducing the solution pH contributes to enhancement in the sorption rate of anions, for example, Cr^{6+} metal ions. This is due to electrostatic interactions between the negative charges of the chromate ion with the positive charge of the adsorbent functional group at low pH. On the contrary, by eliminating Cr^{6+}, raising the pH was stated to contribute to lessening the chromium sorption on the adsorbent surface. This was due to the OH competition with Cr^{6+} species to bind to the active sites at the surface of BC. Therefore, the Cr^{6+} removal was governed by the pH, as presented by Shang et al. (2017). The solution pH also influences the sorption rate of organic pollutants in industrially contaminated water. The sorption of dyes in contaminated water with BC obtained from food residue was examined (Parshetti et al., 2013). They noticed that an alkaline pH improved the sorption of dyes in polluted water. It was due to the strong association between the positively charged dyes with the negatively charged adsorbent surface. Contrastingly, at pH 3, its capacity to remove organic dye is reduced due to the presence of extra hydrogen ions that compete with the positive charges of the dye. Xu et al. (2011) and Tsai and Chen (2013) described similar results on the influence of the pH on the sorption efficiency of adsorbent. Consequently, the solution pH affects the sorption efficiency of inorganic compounds, antibiotics, and other organic contaminants from contaminated water on BC by modifying the charged sites.

Temperature

The reaction temperature is an important parameter affecting the reaction rate and process (Tan et al., 2016a). Most studies have stated that the contaminant adsorption *via* BCs appeared to be an endothermic process and the sorption capacity improved with increasing temperature (Chen et al., 2011; Xu et al., 2011; Parshetti et al., 2013; Vitela-Rodriguez and Rangel-Mendez, 2013; Parshetti et al., 2014; Tan et al., 2016b; Lu et al., 2017; Wang et al., 2018). Meng et al. (2014) examined the influence of different temperatures on the adsorption of Cu^{2+} using swine manure BC, and thermodynamic results were evaluated. The positive values of ΔH showed that the process was endothermic (Meng et al., 2014). Parshetti et al. (2014) investigated the adsorption of dyes using BC derived from food residue at 20°C, 30°C, and 40°C. Positive values of ΔH and negative values of ΔG^{o} showed that dye adsorption on BC was endothermic and spontaneous. The enhancement in the absolute values of ΔG^{o} with the temperature rise proposed that dye adsorption on BC was more favorable at high temperatures. Liu and Zhang (2009) presented that high temperature favored the adsorption of Pb^{+} onto rice husk and pinewood BC. The higher temperature provided adequate energy for Pb^{+} to be seized onto the interior structure of the adsorbent (Liu and Zhang, 2009). Sun et al. (2013) examined the influence of different temperatures (30°C, 40°C, and 50°C) on methylene blue adsorption using BC derived from *Eucalyptus*. The results revealed that the influence of temperature on the sorption efficiency of methylene blue was substantially increased for *Eucalyptus*-derived adsorbent with the temperature rising to 50°C. This effect probably occurred due to the increased diffusion rate of methylene blue with rising temperature (Sun et al., 2013). In general, the reaction conditions, such as cation net release concentration, solution pH, and removal capacity of Cd^{2+} after equilibrium, are similar at various temperatures without remarkable differences (Tan et al., 2016a). When equilibrium temperature does not substantially affect the sorption mechanism, it proposes that the sorption is of a chemical nature instead of physical (Vitela-Rodriguez and Rangel-Mendez, 2013).

Adsorbent dose

The adsorbent amount is a significant parameter influencing the removal efficiency (Deveci and Kar, 2013; Zhang et al., 2013). The adsorption efficiency is also influenced by the dose of adsorbent. Chen et al. (2011) examined the removal of metals such as Zn, Pb, Cu, and Cd from contaminated water with BC obtained from corn straw and hardwood. They found an enhancement of the adsorption rate of the target metals when

the BC amount/dose increased from 0.5 to 5 g/L. It was due to enhancement in the surface area and active sites by increasing the dose of adsorbent. Similar results were presented by Lalhruaitluanga et al. (2010), Tsai and Chen (2013), and Lu et al. (2017). Furthermore, they noticed that increasing the BC dose from 1 to 8 g/L las to enhances the active sites available to remove methylene blue (Sun et al., 2013). Wang et al. (2018) found similar results by increasing the dose of BC for the sorption of organic contaminants. A high amount of adsorbent has a strong effect on the sorption efficiency of toxic metals, antibiotics, and organic contaminants. Therefore, it would be beneficial to obtain the ideal dose/amount, which is a key factor in minimizing the BC fabrication costs because of its application (Wang et al., 2018).

Mechanisms responsible for the removal of pollutants

Mechanisms involved in the adsorption of antibiotics and other organic pollutants

Several mechanisms are involved in pollutant removal from water using BC and engineered BCs, such as π–π EDA interaction, electrostatic interaction, partitioning, hydrophobic interaction, and pore-filling.

Electrostatic interaction

Electrostatic interaction is the most significant mechanism, which accelerates the adsorption of antibiotics and organic pollutants to the positively charged surface of the adsorbents by electrostatic interaction. Its ability to repel or attract contaminants depends on ionic strength and solution pH (Ahmad et al., 2014). This can accelerate electrostatic interaction between the anionic or cationic forms of pollutants and the pristine/modified-composite surface. Such electrostatic interactions have been observed in several studies, for example, on the norfloxacin adsorption by attapulgite–BC composite (Li H. et al., 2017), phosphate adsorption *via* montmorillonite-modified BC (Chen et al., 2017), and arsenic adsorption by hematite–BC composite (Wang S. et al., 2015). Inyang et al. (2014) reported that the methylene blue removal *via* the CNT–BC composite exhibited that the enhancement of ionic strength of the adsorbate solution from 0.01 to 0.1 M NaCl resulted in decreasing the methylene blue adsorption from 4.5 to 3 mg g^{-1}. This was due to an increase in the repulsive electrostatic interaction between the sorbate and sorbent.

Pore-filling

The porous structure of BC surfaces alleviates the adsorption of antibiotics and other organic pollutants by a pore-filling process. During the modification mechanism, the deposition of modifying agents on BC enhances the surface area of BC, thereby increasing the amount of adsorbates that can be adsorbed on the surface (Li M. et al., 2017). The pore-filling process depends on the polarity of antibiotics and organic pollutants, as well as the type and nature of the adsorbent. Kasozi et al. (2010) stated that BC obtained from gamma loblolly, oak, and grass for the catechol adsorption using the micro-pore-filling mechanism is more prevalent than other sorption mechanisms. Generally, to have great effectiveness from this pore-filling mechanism, the adsorbent must contain a slight quantity of volatile matter and occur at low concentrations of antibiotics and organic pollutants (Kasozi et al., 2010).

Partitioning

In this mechanism, the sorbate material diffuses into the pores of the non-carbonized part of the adsorbent. This part can easily interact with the organic pollutant leading to its adsorption. Nonetheless, the organic contaminant adsorption depends on the properties of the non-carbonized BC (amorphous or crystalline C) and carbonized graphene and crystalline fractions of the BC. Zhang et al. (2013) presented that BC obtained from dairy and swine manure exhibited great sorbate partitioning of atrazine contaminant employing organic C fractions of the BC. Similar findings were noticed by Sun et al. (2011), exhibiting that organic fractions of BC produced from grass and wood can increase the fluridone and norflurazon adsorption *via* a partitioning mechanism. Generally, the partitioning process is highly efficient and more visible when the BC has high volatile matter content and a higher amount of organic pollutants (Keiluweit et al., 2010).

Hydrophobic interaction

This process can be employed for the neutral and hydrophobic organic contaminants adsorption *via* the hydrophobic interaction and partitioning mechanisms. When contrasted with the partitioning mechanism, the hydrophobic interaction process needs less energy. Furthermore, the main mechanism for organic pollutant adsorption on the surface of the graphene structure is the hydrophobic interaction (Zhu et al., 2005). Li et al. (2018) presented similar results; the hydrophobic interaction is the key process involved in the sorption of ionizable-organic impurities such as p-chlorobenzene acid, o-chlorobenzene acid, and benzoic acid (Li Y. et al., 2017). Chen et al. (2011) examined the sorption of perfluoro-octane-sulfonic acid on BC derived from corn straw. The sorption occurred by the hydrophobic interaction due to the strong hydrophobic nature of the pollutant. The sorption of perfluoro-octane-sulfonic molecules improved with enhancement in the production temperature. This was ascribed to the reduction in the number of polar groups on the surface of BC caused by the pyrolytic temperature. Sorption mechanisms of inorganic and organic contaminants onto BCs are revealed in Figure 3. Generally, the adsorption of metals on BC occurs by precipitation, electrostatic attraction, and ion exchange onto the BC surface, whereas the sorption

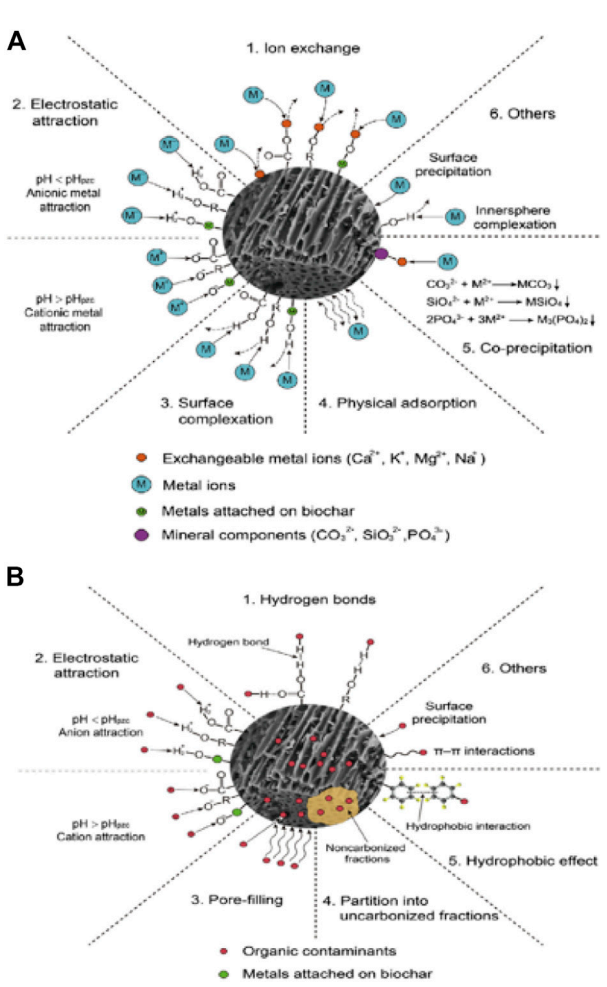

FIGURE 3
Modified/unmodified biochar possible adsorption mechanisms for antibiotic, inorganic, and organic pollutants (adapted from Tang et al., 2015).

mechanisms for antibiotics and organic pollutants are hydrophobic interactions, H-bonding, and van der Waals forces, as presented in Figure 3. The functional groups such as amine, carbonyl, carboxyl, and hydroxyl support the affinity of organic particles and their sorption on the surface of the adsorbent.

EDA interaction

This mechanism is mainly employed for the sorption of aromatic composites on the BC exhibiting a graphene-based structure. In order to have complete graphitization, a temperature higher than 1,000°C should be reached during BC production (Spokas, 2010). Nonetheless, the electron density of BC to create enrichment or deficient π–electron depends on the pyrolytic temperature of BC. If the temperature of BC is less than 500°C, the system of the BC π aromatic performs as the electron acceptor. However, if the temperature exceeds 500°C, the BC works as a donor (Spokas, 2010; Sun et al., 2014). Zheng et al. (2013) examined the sulfamethoxazole adsorption using BC obtained from a reed plant and made enhancement on its surface with π–electron graphene. Great adsorption was noticed between the graphene surface of the adsorbent and aniline-protonated rings of sulfamethoxazole. Moreover, they noticed that the π–electron acceptor/donor attraction between the electron-withdrawing substituent of aromatic carbon and chlorine on the BC surface increases the atrazine compound adsorption.

Mechanisms involved in the adsorption of heavy metals

Several mechanisms are involved in the sorption of heavy metals, such as complexation, precipitation, electrostatic interaction, ion exchange, and surface sorption. The synthesis process of biochar composites, changes in their structure and role in the removal of aquatic pollutants has been clearly described in Figure 4.

Complexation

The metal complexation mechanism serves the arrangement of multi-atom creation *via* the interaction of specific metal ligands to make a complex. At low temperatures, the produced BC can bind with metals because of the O-enriched functional groups, including carboxyl, lactonic, and phenolic. These oxygen-enriched groups can enhance the surface oxidation of BC, contributing to increasing the metal complexation (Ambaye et al., 2021). It has been revealed that BC produced from plant biomass has great ability in the binding of metals, for instance, Pb, Ni, Cd, and Cu, to form metal complexes with phenolic and carboxylic groups compared with the BC obtained from poultry litter and animal manure (Cao et al., 2009). They determined that BC derived from plants shows high ion exchange capacities and great surface complexation. However, more studies are required to conclude the formation of BC–metal complexes using spectroscopic techniques, including FTIR and XPS.

Precipitation

The precipitation mechanism can be employed for the adsorption of heavy metals and other inorganic impurities onto BC and BC-based composite. It contributes to the generation of mineral precipitates onto the sorbing material surface, particularly for the adsorbent, which is derived from the degradation of hemicelluloses and cellulose material by production temperature higher than 300°C and having basic/alkaline characteristics (Cao et al., 2009). Puga et al. (2016) described that BC produced from straw dust and sugarcane could increase the precipitation of Zn and Cd. Nonetheless, they concluded that the capability of BC surface precipitation

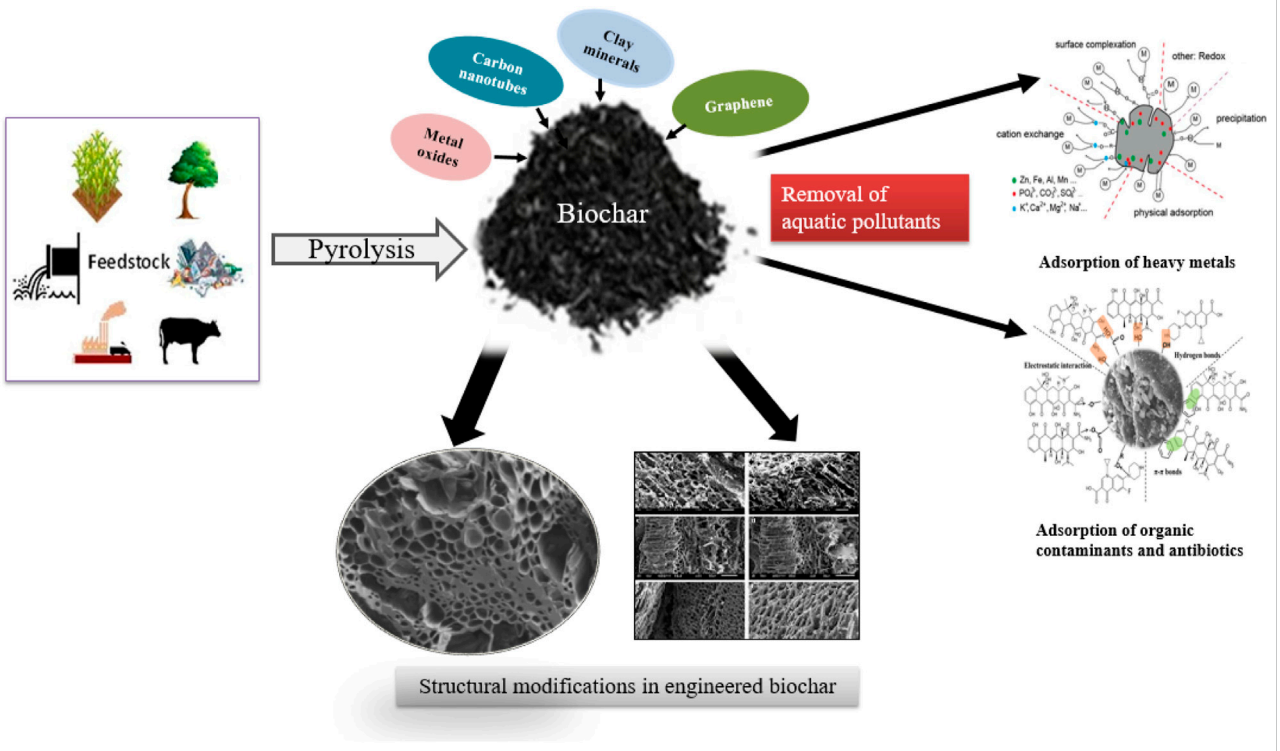

FIGURE 4
Preparation process of biochar-based engineered composites and their implications for removing aquatic pollutants.

depends on the preparation temperature of BC. Thus, further studies are required in the future on the optimization of the pyrolytic temperature.

Ion/cation-exchange capacity

The exchange of ionized cations and protons with dissolved salts on the surface of BC is the key factor of this process. Its adsorption efficiency in eliminating heavy metals and other inorganic impurities depends on the adsorbent surface functional groups and pollutants size (Rizwan et al., 2016). The greater the cation-exchange capacity of the BC and BC-based composite, the greater the sorption of heavy metals and other inorganic chemicals. Nonetheless, cation-exchange capacity lessens with pyrolytic temperatures higher than 300°C (Rizwan et al., 2016). EL-Shafay (2010) examined the Zn^{2+} and Hg^{2+} removal from contaminated water using rice husk BC; they achieved a higher sorption capacity of Hg^{2+} compared to Zn^{2+}. Trakal et al. (2016) examined the elimination of Pb and Cd using BC derived from a nutshell, plum stone, grape stalk and husk, and wheat straw. The results exhibited the higher Cd and Pb removal capacity for the biomasses comprising iron oxides. The existence of Fe in BC biomass was seen to increase the ion-exchange amount of BC/BC-based composite.

Electrostatic attraction

This process involves the electrostatic attraction between the metal ions and charged BC to limit the mobilization of heavy metals (Agrafioti et al., 2014). For example, the Pb removal from contaminated water using wheat and rice-derived BC/BC-based composite exhibits great removal capacity of Pb because of the attraction of negatively charged BC and positively charged Pb. Additionally, it was found that increasing the pyrolytic temperature above 400°C can increase the BC carbonization and contribute to an increase in the electrostatic attraction of BC to remove the contaminant (Qiu et al., 2009). Similar results were described by Keiluweit et al. (2010), Dong et al. (2011), Mukherjee et al. (2011), Agrafioti et al. (2014), and Igalavithana et al. (2017), who noticed that electrostatic attraction is the key mechanism that contributed to heavy metal adsorption. Nonetheless, this immobilization mechanism depends on the PH_z charge of BC and solution pH.

Surface adsorption (physical process)

This mechanism contributes to generating chemical bonds via metal ion diffusion in the adsorbent pores. The surface area and pore volume of the BC/BC-based composite depend on the pyrolysis temperature (Dong et al., 2011). Kumar et al.

(2017) examined the adsorption of uranium using pinewood BC prepared at 300°C and 700°C. The results exhibited that BC derived at 700°C (high temperature) can greatly adsorb the uranium compared to BC produced at 300°C (low temperature). They concluded that this is because the high carbonization increases the pore volume and surface area of BC (Kumar et al., 2017). Wang M. C. et al. (2015) studied the Cd, Cu, and Pb adsorption using $KMnO_4$-modified hickory wood BC. The BC exhibited the adsorption capacity of Cd, Cu, ad Pb as 28.1, 34.2, and 153.1 mg g^{-1}, respectively. This difference in sorption capacity may be due to the affinity of Cd, Cu, and Pb, showing different valences toward the BC (Wang S. et al., 2015).

Conclusion and future outlooks

This review emphasizes the application of engineered/modified or BC-based composites for the removal and management of organic contaminants, antibiotics, heavy metals, and other inorganic impurities in the aqueous medium. Modification alters surface characteristics of BC, such as functional groups, surface charge, pore size, and volume, as well as surface area. Several modifying agents have been employed combining with BCs such as graphene, polymers, graphene oxide, CNT, ZnVI, metals, and their oxides, as well as clay minerals. In general, the modifiers significantly improve sorption abilities but sometimes negatively affect the sorption capacities of antibiotics and organic and inorganic pollutants. Thus, the best approaches to designing/developing BC-based composite are needed to remove pollutants, such as antibiotics and organic and inorganic impurities, from the environment. Results exhibit that the BC-based composites are efficient in eliminating target pollutants. The efficiency and type of a specific mechanism depend on various factors, mainly on the physicochemical characteristics and composition of the BC-based composites and pollutants such as heavy metals, antibiotics, and organic and other inorganic impurities, as well as on the application conditions. In the case of antibiotics and organic pollutants/adsorbates with an aromatic structure and in the existence of functional groups having the nature of electron donors–acceptors, π–π EDA attraction with the BC surface and hydrophobic attraction are dominant. Among engineered BCs, the performance of clay–BC composites in water decontamination has not been vastly investigated. However, the limited published information provides sufficient proof for the efficiency of clay–BC composites for antibiotic, dye, metal, and nutrient removal. Although the surface area is often decreased due to pore blockage, the combined impact of clay minerals and BC significantly enhances the sorption capacity of BC–clay-modified adsorbents, particularly when layered clays are mixed with BC. Therefore, more studies will be needed to improve the information regarding sorption mechanisms, surface chemistry, and the factors affecting the sorption capabilities of BC–clay adsorbents produced *via* clay minerals. BC modification with metals and their oxides has been investigated in relation to various pollutants. Certain modifying agents negatively affected the sorption of target pollutants, justifying more exploration. Neither raw BC nor BC-based composites have been revealed to increase nutrients such as nitrates and phosphate sorption, which are the leading chemicals responsible for contaminating the water and inducing eutrophication. Therefore, further studies are needed to identify or develop a proper adsorbent for the removal of nitrates and phosphates. In addition to adsorption, pollutant removal by degradation due to BC–metal oxide composite application was attained. Thus, the BC composite exhibited evidence of strengthening the photocatalytic activity of the catalyst. Therefore, future studies should focus on the preparation of engineered BCs, which can be employed for long-term and complete elimination of emerging pollutants.

Author contributions

Original draft: GM and ZA; review and editing: MU, I,A, RI, D-QD, SA, ASA, MIA, JI and MR; resources and supervision: ZA, D-QD, MR, and AT.

Acknowledgments

This research was supported by the National Natural Science Foundation of China (No. NSFC 31760013) and High-Level Talent Recruitment Plan of Yunnan Provinces Young Talents Program. Further, the authors would like to thank the Researchers and Deanship of Scientific Research at Umm Al-Qura University, Makkah, Saudi Arabia for supporting this work by Grant Code: 22UQU4350073DSR08.

Conflict of interest

The authors declare that the research was conducted in the absence of any commercial or financial relationships that could be construed as a potential conflict of interest.

Publisher's note

References

Agrafioti, E., Kalderis, D., and Diamadopoulos, E. (2014). Ca and Fe modified biochars as adsorbents of arsenic and chromium in aqueous solutions. *J. Environ. Manage.* 146, 444–450. doi:10.1016/j.jenvman.2014.07.029

Ahmad, M., Lee, S. S., Rajapaksha, A. U., Vithanage, M., Zhang, M., Cho, J. S., et al. (2013). Trichloroethylene adsorption by pine needle biochars produced at various pyrolysis temperatures. *Bioresour. Technol.* 143, 615–622. doi:10.1016/j.biortech.2013.06.033

Ahmad, M., Rajapaksha, A., Lim, U., Jung, E., Zhang, M., Bolan, N., et al. (2014). Biochar as a sorbent for contaminant management in soil and water: A review. *Chemosphere* 99, 19–33. doi:10.1016/j.chemosphere.2013.10.071

Ahmed, M. B., Zhou, J. L., Ngo, H. H., Guo, W., and Chen, M. (2016). Progress in the preparation and application of modified biochar for improved contaminant removal from water and wastewater. *Bioresour. Technol.* 214, 836–851. doi:10.1016/j.biortech.2016.05.057

Ahmed, M. B., Zhou, J. L., Ngo, H. H., Guo, W., Johir, M. A. H., Sornalingam, K., et al. (2017). Nano-Fe0 immobilized onto functionalized biochar gaining excellent stability during sorption and reduction of chloramphenicol via transforming to reusable magnetic composite. *Chem. Eng. J.* 322, 571–581. doi:10.1016/j.cej.2017.04.063

Almeelbi, T., and Bezbaruah, A. (2012). Aqueous phosphate removal using nanoscale zerovalent iron. *J. Nanopart. Res.* 14, 900. doi:10.1007/s11051-012-0900-y

Amalina, F., Abd Razak, A. S., Krishnan, S., Zularisam, A. W., and Nasrullah, M. (2022). A comprehensive assessment of the method for producing biochar, its characterization, stability, and potential applications in regenerative economic sustainability–a review. *Clean. Mater.* 3, 100045. doi:10.1016/j.clema.2022.100045

Ambaye, T. G., Vaccari, M., van Hullebusch, E. D., Amrane, A., and Rtimi, S. (2021). Mechanisms and adsorption capacities of biochar for the removal of organic and inorganic pollutants from industrial wastewater. *Int. J. Environ. Sci. Technol.* 18, 3273–3294. doi:10.1007/s13762-020-03060-w

Amen, R., Bashir, H., Bibi, I., Shaheen, S. M., Niazi, N. K., Shahid, M., et al. (2020). A critical review on arsenic removal from water using biochar-based sorbents: The significance of modification and redox reactions. *Chem. Eng. J.* 396, 125195. doi:10.1016/j.cej.2020.125195

Amusat, S. O., Kebede, T. G., Dube, S., and Nindi, M. M. (2021). Ball-milling synthesis of biochar and biochar-based nanocomposites and prospects for removal of emerging contaminants: A review. *J. Water Process Eng.* 41, 101993. doi:10.1016/j.jwpe.2021.101993

Aristilde, L., Lanson, B., Miehe-Brendle, J., Marichal, C., and Charlet, L. (2016). Enhanced interlayer trapping of a tetracycline antibiotic within montmorillonite layers in the presence of Ca and Mg. *J. Colloid Interface Sci.* 464, 153–159. doi:10.1016/j.jcis.2015.11.027

Ashiq, A., Adassooriya, N. M., Sarkar, B., Rajapaksha, A. U., Ok, Y. S., and Vithanage, M. (2019). Municipal solid waste biochar-bentonite composite for the removal of antibiotic ciprofloxacin from aqueous media. *J. Environ. Manage.* 236, 428–435. doi:10.1016/j.jenvman.2019.02.006

Benis, K. Z., Damuchali, A. M., Soltan, J., and McPhedran, K. N. (2020). Treatment of aqueous arsenic-A review of biochar modification methods. *Sci. Total Environ.* 739, 139750. doi:10.1016/j.scitotenv.2020.139750

Bridgwater, A. V. (2012). Review of fast pyrolysis of biomass and product upgrading. *Biomass Bioenergy* 38, 68–94. doi:10.1016/j.biombioe.2011.01.048

Cao, X., Ma, L., Gao, B., and Harris, W. (2009). Dairy-manure derived biochar effectively sorbs lead and atrazine. *Environ. Sci. Technol.* 43, 3285–3291. doi:10.1021/es803092k

Chang, P. H., Li, Z., Jean, J. S., Jiang, W. T., Wu, Q., Kuo, C. Y., et al. (2014). Desorption of tetracycline from montmorillonite by aluminum, calcium, and sodium: An indication of intercalation stability. *Int. J. Environ. Sci. Technol.* 11, 633–644. doi:10.1007/s13762-013-0215-2

Chaukura, N., Murimba, E. C., and Gwenzi, W. (2017). Synthesis, characterisation and methyl orange adsorption capacity of ferric oxide–biochar nano-composites derived from pulp and paper sludge. *Appl. Water Sci.* 7, 2175–2186. doi:10.1007/s13201-016-0392-5

Chen, B., Chen, Z., and Lv, S. (2011). A novel magnetic biochar efficiently sorbs organic pollutants and phosphate. *Bioresour. Technol.* 102, 716–723. doi:10.1016/j.biortech.2010.08.067

Chen, B., Zhou, D., and Zhu, L. (2008). Transitional adsorption and partition of nonpolar and polar aromatic contaminants by biochars of pine needles with different pyrolytic temperatures. *Environ. Sci. Technol.* 42, 5137–5143. doi:10.1021/es8002684

Chen, L., Chen, X. L., Zhou, C. H., Yang, H. M., Ji, S. F., Tong, D. S., et al. (2017). Environmental-friendly montmorillonite-biochar composites: Facile production and tunable adsorption-release of ammonium and phosphate. *J. Clean. Prod.* 156, 648–659. doi:10.1016/j.jclepro.2017.04.050

Chen, Y., Shi, J., Du, Q., Zhang, H., and Cui, Y. (2019). Antibiotic removal by agricultural waste biochars with different forms of iron oxide. *RSC Adv.* 9, 14143–14153. doi:10.1039/c9ra01271k

Cruz, G. J. F., Mondal, D., Rimaycuna, J., Soukup, K., Gomez, M. M., Solis, J, L., et al. (2020). Agrowaste derived biochars impregnated with ZnO for removal of arsenic and lead in water. *J. Environ. Chem. Eng.* 8, 103800. doi:10.1016/j.jece.2020.103800

Cui, H., Ou, Y., Wang, L., Yan, B., Li, Y., and Bao, M. (2021). Dissolved organic carbon, a critical factor to increase the bioavailability of phosphorus during biochar-amended aerobic composting. *J. Environ. Sci.* 113, 356–364. doi:10.1016/j.jes.2021.06.019

Deveci, H., and Kar, Y. (2013). Adsorption of hexavalent chromium from aqueous solutions by biochars obtained during biomass pyrolysis. *J. Ind. Eng. Chem.* 19, 190–196. doi:10.1016/j.jiec.2012.08.001

Dhyani, V., and Bhaskar, T. (2018). A comprehensive review on the pyrolysis of lignocellulosic biomass. *Renew. Energy* 129, 695–716. doi:10.1016/j.renene.2017.04.035

Di Blasi, C. (2008). Modeling chemical and physical processes of wood and biomass pyrolysis. *Prog. Energy Combust. Sci.* 34, 47–90. doi:10.1016/j.pecs.2006.12.001

Ding, W., Dong, X., Ime, I. M., Gao, B., and Ma, L. Q. (2014). Pyrolytic temperatures impact lead sorption mechanisms by bagasse biochars. *Chemosphere* 105, 68–74. doi:10.1016/j.chemosphere.2013.12.042

Domingues, R. R., Trugilho, P. F., Silva, C. A., de Melo, I. C. N. A., Melo, L. C. A., Magriotis, Z. M., et al. (2017). Properties of biochar derived from wood and high-nutrient biomasses with the aim of agronomic and environmental benefits. *PLoS One* 12, e0176884. doi:10.1371/journal.pone.0176884

Dong, X., Ma, L. Q., and Li, Y. (2011). Characteristics and mechanisms of hexavalent chromium removal by biochar from sugar beet tailing. *J. Hazard. Mat.* 190, 909–915. doi:10.1016/j.jhazmat.2011.04.008

Duan, C., Ma, T., Wang, J., and Zhou, Y. (2020). Removal of heavy metals from aqueous solution using carbon-based adsorbents: A review. *J. Water Process Eng.* 37, 101339. doi:10.1016/j.jwpe.2020.101339

Duwiejuah, A. B., Abubakari, A. H., Quainoo, A. K., and Amadu, Y. (2020). Review of biochar properties and remediation of metal pollution of water and soil. *J. Health Pollut.* 10, 200902. doi:10.5696/2156-9614-10.27.200902

El-Shafey, E. I. (2010). Removal of Zn(II) and Hg(II) from aqueous solution on a carbonaceous sorbent chemically prepared from rice husk. *J. Hazard. Mat.* 175, 319–327. doi:10.1016/j.jhazmat.2009.10.006

Essandoh, M., Wolgemuth, D., Pittman, C. U., Mohan, D., and Mlsna, T. (2017). Adsorption of metribuzin from aqueous solution using magnetic and nonmagnetic sustainable low-cost biochar adsorbents. *Environ. Sci. Pollut. Res.* 24, 4577–4590. doi:10.1007/s11356-016-8188-6

Feng, Y., Liu, P., Wang, Y., Finfrock, Y. Z., Xie, X., Su, C., et al. (2019). Distribution and speciation of iron in Fe-modified biochars and its application in removal of As(V), As(III), Cr(VI), and Hg(II): An X-ray absorption study. *J. Hazard. Mat.* 384, 121342. doi:10.1016/j.jhazmat.2019.121342

Fosso-Kankeu, E., Waanders, F. B., and Steyn, F. W. (2015). "The preparation and characterization of clay-biochar composites for the removal of metal pollutants," in 7th International Conference on Latest Trends in Engineering & Technology Irene, Eartscan, United Kingdom (Pretoria, South Africa: Lehman and Joseph.

Fosso-Kankeu, E., Waanders, F. B., and Steyn, F. W. (2016). "Enhanced Adsorption Capacity of Sweet Sorghum Derived Biochar towards Malachite Green Dye Using Bentonite Clay," in Int'l Conf. on Advances in Science, Engineering, Technology and Natural Resources (ICASETNR-16), November 24–25, 2016, Parys (South Africa).

Fristak, V., Michalekova-Richveisova, B., Viglasova, E., Duriska, L., Galambos, M., Moreno-Jimenez, E., et al. (2017). Sorption separation of Eu and as from single-component systems by Fe-modified biochar: Kinetic and equilibrium study. *J. Iran. Chem. Soc.* 14, 521–530. doi:10.1007/s13738-016-1000-1

Fuertes, A. B., Camps Arbestain, M., Sevilla, M., Macia-Agullo, J. A., Fiol, S., Lopez, R., et al. (2010). Chemical and structural properties of carbonaceous products obtained by pyrolysis and hydrothermal carbonisation of corn stover. *Soil Res.* 48, 618–626. doi:10.1071/sr10010

Gai, X., Wang, H., Liu, J., Zhai, L., Liu, S., Ren, T., et al. (2014). Effects of feedstock and pyrolysis temperature on biochar adsorption of ammonium and nitrate. *PLoS One* 9, e113888. doi:10.1371/journal.pone.0113888

Gao, Y., Li, Y., Zhang, L., Huang, H., Hu, J., Shah, S. M., et al. (2015). Adsorption and removal of tetracycline antibiotics from aqueous solution by graphene oxide. *J. Colloid Interface Sci.* 368, 540–546. doi:10.1016/j.jcis.2011.11.015

Ghaffar, A., and Younis, M. N. (2014). Adsorption of organic chemicals on graphene coated biochars and its environmental implications. *Green Process. Synthesis* 3, 479–487. doi:10.1515/gps-2014-0071

Godlewska, P., Bogusz, A., Dobrzynska, J., Dobrowolski, R., and Oleszczuk, P. (2020). Engineered biochar modified with iron as a new adsorbent for treatment of water contaminated by selenium. *J. Saudi Chem. Soc.* 24, 824–834. doi:10.1016/j.jscs.2020.07.006

Han, L., Xue, S., Zhao, S., Yan, J., Qian, L., and Chen, M. (2015). Biochar supported nanoscale iron particles for the efficient removal of methyl orange dye in aqueous solutions. *PLoS One* 10, e0132067. doi:10.1371/journal.pone.0132067

Han, X., Liang, C. F., Li, T. Q., Wang, K., Huang, H. G., and Yang, X. E. (2013). Simultaneous removal of cadmium and sulfamethoxazole from aqueous solution by rice straw biochar. *J. Zhejiang Univ. Sci. B* 14, 640–649. doi:10.1631/jzus.b1200353

Hassan, M., Liu, Y., Naidu, R., Parikh, S. J., Du, J., Qi, F., et al. (2020). Influences of feedstock sources and pyrolysis temperature on the properties of biochar and functionality as adsorbents: A meta-analysis. *Sci. Total Environ.* 744, 140714. doi:10.1016/j.scitotenv.2020.140714

Heo, J., Yoon, Y., Lee, G., Kim, Y., Han, J., and Park, C. M. (2019). Enhanced adsorption of bisphenol A and sulfamethoxazole by a novel magnetic $CuZnFe_2O_4$-biochar composite. *Bioresour. Technol.* 281, 179–187. doi:10.1016/j.biortech.2019.02.091

Hong, S. H., Lyonga, F. N., Kang, J. K., Seo, E. J., Lee, C. G., Jeong, S., et al. (2020). Synthesis of Fe-impregnated biochar from food waste for Selenium (IV) removal from aqueous solution through adsorption: Process optimization and assessment. *Chemosphere* 252, 126475. doi:10.1016/j.chemosphere.2020.126475

Hornung, A. (2014). *Transformation of biomass: Theory to practice*. United Kingdom: Wiley.

Hu, P., Zhang, Y., Liu, L., Wang, X., Luan, X., Ma, X., et al. (2019). Biochar/struvite composite as a novel potential material for slow release of N and P. *Environ. Sci. Pollut. Res.* 26, 17152–17162. doi:10.1007/s11356-019-04458-x

Huang, D., Wang, X., Zhang, C., Zeng, G., Peng, Z., Zhou, J., et al. (2017). Sorptive removal of ionizable antibiotic sulfamethazine from aqueous solution by graphene oxide-coated biochar nanocomposites: Influencing factors and mechanism. *Chemosphere* 186, 414–421. doi:10.1016/j.chemosphere.2017.07.154

Igalavithana, A. D., Mandal, S., Niazi, N. K., Vithanage, M., Parikh, S. J., Mukome, F. N., et al. (2017). Advances and future directions of biochar characterization methods and applications. *Crit. Rev. Environ. Sci. Technol.* 47, 2275–2330. doi:10.1080/10643389.2017.1421844

Inyang, M., Gao, B., Zimmerman, A., Zhang, M., and Chen, H. (2014). Synthesis, characterization, and dye sorption ability of carbon nanotube–biochar nanocomposites. *Chem. Eng. J.* 236, 39–46. doi:10.1016/j.cej.2013.09.074

Inyang, M., Gao, B., Zimmerman, A., Zhou, Y., and Cao, X. (2015). Sorption and cosorption of lead and sulfapyridine on carbon nanotube-modified biochars. *Environ. Sci. Pollut. Res.* 22, 1868–1876. doi:10.1007/s11356-014-2740-z

Inyang, M. I., Gao, B., Yao, Y., Xue, Y., Zimmerman, A., Mosa, A., et al. (2016). A review of biochar as a low-cost adsorbent for aqueous heavy metal removal. *Crit. Rev. Environ. Sci. Technol.* 46, 406–433. doi:10.1080/10643389.2015.1096880

Jafri, N., Wong, W. Y., Doshi, Y., Yoon, L. W., and Cheah, K. H. (2018). A review on production and characterization of biochars for application in direct carbon fuel cells. *Process Saf. Environ. Prot.* 118, 152–166. doi:10.1016/j.psep.2018.06.036

Janu, R., Mrlik, V., Ribitsch, D., Hofman, J., Sedlacek, P., Bielska, L., et al. (2021). Biochar surface functional groups as affected by biomass feedstock, biochar composition and pyrolysis temperature. *Carbon Resour. Convers.* 4, 36–46. doi:10.1016/j.crcon.2021.01.003

Jayathilake, M., Rudra, S., Akhtar, N., and Christy, A. A. (2021). Characterization and evaluation of hydrothermal liquefaction char from alkali lignin in subcritical temperatures. *Materials* 14, 3024. doi:10.3390/ma14113024

Jing, X. R., Wang, Y. Y., Liu, W. J., Wang, Y. K., and Jiang, H. (2014). Enhanced adsorption performance of tetracycline in aqueous solutions by methanol-modified biochar. *Chem. Eng. J.* 248, 168–174. doi:10.1016/j.cej.2014.03.006

Johansson, C. L., Paul, N. A., de Nys, R., and Roberts, D. A. (2016). Simultaneous biosorption of selenium, arsenic and molybdenum with modified algal-based biochars. *J. Environ. Manage.* 165, 117–123. doi:10.1016/j.jenvman.2015.09.021

Joseph, S., Cowie, A. L., Van Zwieten, L., Bolan, N., Budai, A., Buss, W., et al. (2021). How biochar works, and when it doesn't: A review of mechanisms controlling soil and plant responses to biochar. *GCB Bioenergy* 13, 1731–1764. doi:10.1111/gcbb.12885

Kasozi, G. N., Zimmerman, A. R., Nkedi-Kizza, P., and Gao, B. (2010). Catechol and humic acid sorption onto a range of laboratory-produced black carbons (biochars). *Environ. Sci. Technol.* 44, 6189–6195. doi:10.1021/es1014423

Keiluweit, M., Nico, P. S., Johnson, M. G., and Kleber, M. (2010). Dynamic molecular structure of plant biomass-derived black carbon (biochar). *Environ. Sci. Technol.* 44, 1247–1253. doi:10.1021/es9031419

Kirmizakis, P., Tawabini, B., Siddiq, O. M., Kalderis, D., Ntarlagiannis, D., and Soupios, P. (2022). Adsorption of arsenic on Fe-modified biochar and monitoring using spectral induced polarization. *Water* 14, 563. doi:10.3390/w14040563

Kolodynska, D., and Bak, J. (2017). Use of three types of magnetic biochar in the removal of copper (II) ions from wastewaters. *Sep. Sci. Technol.* 53, 1045–1057. doi:10.1080/01496395.2017.1345944

Komnitsas, K., and Zaharaki, D. (2016). Morphology of modified biochar and its potential for phenol removal from aqueous solutions. *Front. Environ. Sci.* 4, 26. doi:10.3389/fenvs.2016.00026

Komnitsas, K., Zaharaki, D., Pyliotis, I., Vamvuka, D., and Bartzas, G. (2015). Assessment of pistachio shell biochar quality and its potential for adsorption of heavy metals. *Waste Biomass Valor.* 6, 805–816. doi:10.1007/s12649-015-9364-5

Krasucka, P., Pan, B., SikOk, Y., Mohan, D., Sarkar, B., and Oleszczuk, P. (2020). Engineered biochar - a sustainable solution for the removal of antibiotics from water. *Chem. Eng. J.* 405, 126926. doi:10.1016/j.cej.2020.126926

Kumar, A., Kumar, A., Sharma, G., Naushad, M., Stadler, F. J., Ghfar, A. A., et al. (2017). Sustainable nano-hybrids of magnetic biochar supported g-C_3N_4/$FeVO_4$ for solar-powered degradation of noxious pollutants-Synergism of adsorption, photocatalysis and photo-ozonation. *J. Clean. Prod.* 165, 431–451. doi:10.1016/j.jclepro.2017.07.117

Kumar, R., Laskar, M. A., Hewaidy, I. F., and Barakat, M. A. (2019). Modified adsorbents for removal of heavy metals from aqueous environment: A review. *Earth Syst. Environ.* 3, 83–93. doi:10.1007/s41748-018-0085-3

Lalhruaitluanga, H., Jayaram, K., Prasad, M. N. V., and Kumar, K. K. (2010). Lead (II) adsorption from aqueous solutions by raw and activated charcoals of Melocanna baccifera Roxburgh (bamboo)-a comparative study. *J. Hazard. Mat.* 175, 311–318. doi:10.1016/j.jhazmat.2009.10.005

Lata, S., and Samadder, S. R. (2016). Removal of arsenic from water using nano adsorbents and challenges: A review. *J. Environ. Manage.* 166, 387–406. doi:10.1016/j.jenvman.2015.10.039

Le Bars, M., Legros, S., Levard, C., Chaurand, P., Tella, M., Rovezzi, M., et al. (2018). Drastic change in zinc speciation during anaerobic digestion and composting: Instability of nanosized zinc sulfide. *Environ. Sci. Technol.* 52, 12987–12996. doi:10.1021/acs.est.8b02697

Lee, H. W., Kim, Y. M., Kim, S., Ryu, C., Park, S. H., and Park, Y. K. (2018). Review of the use of activated biochar for energy and environmental applications. *Carb. Lett.* 26, 1–10. doi:10.5714/CL.2018.26.001

Lee, X. J., Lee, L. Y., Gan, S., Thangalazhy-Gopakumar, S., and Ng, H. K. (2017). Biochar potential evaluation of palm oil wastes through slow pyrolysis: Thermochemical characterization and pyrolytic kinetic studies. *Bioresour. Technol.* 236, 155–163. doi:10.1016/j.biortech.2017.03.105

Legros, S., Levard, C., Marcato-Romain, C. E., Guiresse, M., and Doelsch, E. (2017). Anaerobic digestion alters copper and zinc speciation. *Environ. Sci. Technol.* 51, 10326–10334. doi:10.1021/acs.est.7b01662

Lehmann, J., and Joseph, S. (2009). *Biochar for environmental management: Science and Technology*. Earthscan, UK.

Li, G., Shen, B., Li, F., Tian, L., Singh, S., and Wang, F. (2015). Elemental mercury removal using biochar pyrolyzed from municipal solid waste. *Fuel Process. Technol.* 133, 43–50. doi:10.1016/j.fuproc.2014.12.042

Li, H., Dong, X., da Silva, E. B., de Oliveira, L. M., Chen, Y., and Ma, L. Q. (2017). Mechanisms of metal sorption by biochars: Biochar characteristics and modifications. *Chemosphere* 178, 466–478. doi:10.1016/j.chemosphere.2017.03.072

Li, M., Zhao, Z., Wu, X., Zhou, W., and Zhu, L. (2017). Impact of mineral components in cow manure biochars on the adsorption and competitive adsorption of oxytetracycline and carbaryl. *RSC Adv.* 7, 2127–2136. doi:10.1039/c6ra26534k

Li, R., Wang, Z., Zhao, X., Li, X., and Xie, X. (2018). Magnetic biochar-based manganese oxide composite for enhanced fluoroquinolone antibiotic removal from water. *Environ. Sci. Pollut. Res.* 25, 31136–31148. doi:10.1007/s11356-018-3064-1

Li, X., Wang, C., Zhang, J., Liu, J., Liu, B., and Chen, G. (2019). Preparation and application of magnetic biochar in water treatment: A critical review. *Sci. Total Environ.* 177, 134847. doi:10.1016/j.scitotenv.2019.134847

Li, Y., Wang, Z., Xie, X., Zhu, J., Li, R., and Qin, T. (2017). Removal of Norfloxacin from aqueous solution by clay-biochar composite prepared from potato stem and natural attapulgite. *Colloids Surfaces A Physicochem. Eng. Aspects* 514, 126–136. doi:10.1016/j.colsurfa.2016.11.064

Li, J. Q., Nie, M., and Pendall, E. (2020). Soil physico-chemical properties are more important than microbial diversity and enzyme activity in controlling carbon and nitrogen stocks near Sydney. *Aust. Geoderma* 366, 114201. doi:10.1016/j.geoderma.2020.114201

Lian, F., Huang, F., Chen, W., Xing, B., and Zhu, L. (2011). Sorption of apolar and polar organic contaminants by waste tire rubber and its chars in single-and

bi-solute systems. *Environ. Pollut.* 159, 850–857. doi:10.1016/j.envpol.2011.01.002

Liang, C., Gasco, G., Fu, S., Mendez, A., and Paz-Ferreiro, J. (2016). Biochar from pruning residues as a soil amendment: Effects of pyrolysis temperature and particle size. *Soil Tillage Res.* 164, 3–10. doi:10.1016/j.still.2015.10.002

Liang, H., Zhu, C., Ji, S., Kannan, P., and Chen, F. (2022). Magnetic Fe_2O_3/biochar composite prepared in a molten salt medium for antibiotic removal in water. *Biochar* 4, 3. doi:10.1007/s42773-021-00130-1

Liang, L., Xi, F., Tan, W., Meng, X., Hu, B., and Wang, X. (2021). Review of organic and inorganic pollutants removal by biochar and biochar-based composites. *Biochar* 3, 255–281. doi:10.1007/s42773-021-00101-6

Ling, L. L., Liu, W. J., Zhang, S., and Jiang, H. (2017). Magnesium oxide embedded nitrogen selfdoped biochar composites: Fast and high-efficiency adsorption of heavy metals in an aqueous solution. *Environ. Sci. Technol.* 51, 10081–10089. doi:10.1021/acs.est.7b02382

Liu, T., Gao, B., Fang, J., Wang, B., and Cao, X. (2016). Biochar-supported carbon nanotube and graphene oxide nanocomposites for Pb(II) and Cd(II) removal. *RSC Adv.* 6, 24314–24319. doi:10.1039/c6ra01895e

Liu, W. J., Jiang, H., and Yu, H. Q. (2015). Development of biochar-based functional materials: Toward a sustainable platform carbon material. *Chem. Rev.* 115, 12251–12285. doi:10.1021/acs.chemrev.5b00195

Liu, Y., Sohi, S. P., Liu, S., Guan, J., Zhou, J., and Chen, J. (2019). Adsorption and reductive degradation of Cr (VI) and TCE by a simply synthesized zero valent iron magnetic biochar. *J. Environ. Manage.* 235, 276–281. doi:10.1016/j.jenvman.2019.01.045

Liu, Z., and Zhang, F. S. (2009). Removal of lead from water using biochars prepared from hydrothermal liquefaction of biomass. *J. Hazard. Mat.* 167, 933–939. doi:10.1016/j.jhazmat.2009.01.085

Lou, K., Rajapaksha, A. U., Ok, Y. S., and Chang, S. X. (2016). Pyrolysis temperature and steam activation effects on sorption of phosphate on pine sawdust biochars in aqueous solutions. *Chem. Speciat. Bioavailab.* 28, 42–50. doi:10.1080/09542299.2016.1165080

Lu, H., Zhang, W., Yang, Y., Huang, X., Wang, S., and Qiu, R. (2012). Relative distribution of Pb^{2+} sorption mechanisms by sludge-derived biochar. *Water Res.* 46, 854–862. doi:10.1016/j.watres.2011.11.058

Lu, K., Yang, X., Gielen, G., Bolan, N., Ok, Y. S., Niazi, N. K., et al. (2017). Effect of bamboo and rice straw biochars on the mobility and redistribution of heavy metals (Cd, Cu, Pb and Zn) in contaminated soil. *J. Environ. Manage.* 186, 285–292. doi:10.1016/j.jenvman.2016.05.068

Lupoi, J. S., and Smith, E. A. (2012). Characterization of woody and herbaceous biomasses lignin composition with 1064 nm dispersive multichannel Raman spectroscopy. *Appl. Spectrosc.* 66, 903–910. doi:10.1366/12-06621

Ma, Y., Li, P., Yang, L., Wu, L., He, L., Gao, F., et al. (2020). Iron/zinc and phosphoric acid modified sludge biochar as an efficient adsorbent for fluoroquinolones antibiotics removal. *Ecotoxicol. Environ. Saf.* 196, 110550. doi:10.1016/j.ecoenv.2020.110550

Mandal, S., Sarkar, B., Bolan, N., Novak, J., Ok, Y. S., Van Zwieten, L., et al. (2016). Designing advanced biochar products for maximizing greenhouse gas mitigation potential. *Crit. Rev. Environ. Sci. Technol.* 46, 1367–1401. doi:10.1080/10643389.2016.1239975

Meng, J., Feng, X., Dai, Z., Liu, X., Wu, J., and Xu, J. (2014). Adsorption characteristics of Cu (II) from aqueous solution onto biochar derived from swine manure. *Environ. Sci. Pollut. Res.* 21, 7035–7046. doi:10.1007/s11356-014-2627-z

Mia, S., Singh, B., and Dijkstra, F. A. (2017). Aged biochar affects gross nitrogen mineralization and recovery; A 15 N study in two contrasting soils. *GCB Bioenergy* 9, 1196–1206. doi:10.1111/gcbb.12430

Miyajima, K., and Noubactep, C. (2012). Effects of mixing granular iron with sand on the efficiency of methylene blue discoloration. *Chem. Eng. J.* 200-202, 433–438. doi:10.1016/j.cej.2012.06.069

Mohan, D., Sarswat, A., Ok, Y. S., and Pittman, C. U. (2014). Organic and inorganic contaminants removal from water with biochar, a renewable, low cost and sustainable adsorbent - a critical review. *Bioresour. Technol.* 160, 191–202. doi:10.1016/j.biortech.2014.01.120

Mukherjee, A., Zimmerman, A. R., and Harris, W. (2011). Surface chemistry variations among a series of laboratory-produced biochars. *Geoderma* 163, 247–255. doi:10.1016/j.geoderma.2011.04.021

Mukome, F. N. D., Zhang, X., Lucas, C. R. S., Six, J., and Parikh, S. J. (2013). Use of chemical and physical characteristics to investigate trends in biochar feedstocks. *J. Agric. Food Chem.* 61, 2196–2204. doi:10.1021/jf3049142

Murtaza, G., Ahmed, Z., Usman, M., Areeb, A., Ditta, A., Ullah, Z., et al. (2020). Impacts on biochar aging mechanism by eco-environmental factors. *Proc. Int. Acad. Ecol. Environ. Sci.* 10, 97–104.

Murtaza, G., Ahmed, Z., Usman, M., Ditta, A., Ullah, Z., Shabbir, N., et al. (2021c). Future research perspectives of biochar and electrical characteristics of charcoal. *Proc. Int. Acad. Ecol. Environ. Sci.* 11, 1–15.

Murtaza, G., Ahmed, Z., and Usman, M. (2022). Feedstock type, pyrolysis temperature and acid modification effects on physiochemical attributes of biochar and soil quality. *Arab. J. Geosci.* 15, 305. doi:10.1007/s12517-022-09539-9

Murtaza, G., Ahmed, Z., Usman, M., Tariq, W., Ullah, Z., Shareef, M., et al. (2021a). Biochar induced modifications in soil properties and its impacts on crop growth and production. *J. Plant Nutr.* 44, 1–15. doi:10.1080/01904167.2021.1871746

Murtaza, G., Ditta, A., Ullah, N., Usman, M., and Ahmed, Z. (2021b). Biochar for the management of nutrient impoverished and metal contaminated soils: Preparation, applications, and prospects. *J. Soil Sci. Plant Nutr.* 21, 2191–2213. doi:10.1007/s42729-021-00514-z

Nazir, M. S., Kassim, M. H., Mohapatra, L., Gilani, M. A., Raza, M. R., and Majeed, K. (2016). "Characteristic properties of manoclays and characterization of nanoparticulates and nanocomposites," in *Nanoclay reinforced polymer composites: Nanocomposites and bionanocomposites*. Editors M. Jawaid, A. E. K. Qaiss, and R. Bouhfid (Singapore: Springer Singapore), 35–55.

Nham, N. T., Al Tahtamouni, T. M., Nguyen, T. D., Thi Huong, P., Kim, J., Viet, N. M., et al. (2019). Synthesis of iron modified rice straw biochar toward arsenic from groundwater. *Mat. Res. Express* 6, 115528. doi:10.1088/2053-1591/ab4b98

Novak, J. M., Lima, I., Xing, B., Gaskin, J. W., Steiner, C., Das, K. C., et al. (2009). Characterization of designer biochar produced at different temperatures and their effects on loamy sand. *Ann. Environ. Sci.* 3, 195–206.

O'Connor, D., Peng, T., Li, G., Wang, S., Duan, L., Mulder, J., et al. (2018). Sulfur-modified rice husk biochar: A green method for the remediation of mercury contaminated soil. *Sci. Total Environ.* 621, 819–826. doi:10.1016/j.scitotenv.2017.11.213

Ok, Y. S., Uchimiya, S. M., Chang, S. X., and Bolan, N. (2015). Biochar-production, characterization and applications. *CRC Press*. London: Taylor and Francis. doi:10.1201/b18920

Ooi, C. H., Sim, Y. L., and Yeoh, F. Y. (2017). Urea adsorption by activated carbon prepared from palm kernel shell. *AIP. Conf. Proc.* 1865, 020009. doi:10.1063/1.4993328

Parshetti, G. K., Chowdhury, S., and Balasubramanian, R. (2014). Hydrothermal conversion of urban food waste to chars for removal of textile dyes from contaminated waters. *Bioresour. Technol.* 161, 310–319. doi:10.1016/j.biortech.2014.03.087

Parshetti, G. K., Hoekman, S. K., and Balasubramanian, R. (2013). Chemical, structural and combustion characteristics of carbonaceous products obtained by hydrothermal carbonization of palm empty fruit bunches. *Bioresour. Technol.* 135, 683–689. doi:10.1016/j.biortech.2012.09.042

Peiris, C., Gunatilake, S. R., Mlsna, T. E., Mohan, D., and Vithanage, M. (2017). Biochar based removal of antibiotic sulfonamides and tetracyclines in aquatic environments: A critical review. *Bioresour. Technol.* 246, 150–159. doi:10.1016/j.biortech.2017.07.150

Pokharel, A., Acharya, B., and Farouque, A. (2020). "Biochar-assisted wastewater treatment and waste valorization," in *Applications of biochar for environmental safety*. Editors A. Abdelhafez and M. Abbas. Switzeland: Springer Nature, 356.

Pous, N., Casentini, B., Rossetti, S., Fazi, S., Puig, S., and Aulenta, F. (2015). Anaerobic arsenite oxidation with an electrode serving as the sole electron acceptor: A novel approach to the bioremediation of arsenic-polluted groundwater. *J. Hazard. Mat.* 283, 617–622. doi:10.1016/j.jhazmat.2014.10.014

Premarathna, K. S. D., Rajapaksha, A. U., Adassoriya, N., Sarkar, B., Sirimuthu, N. M. S., Cooray, A., et al. (2019a). Clay-biochar composites for sorptive removal of tetracycline antibiotic in aqueous media. *J. Environ. Manage.* 238, 315–322. doi:10.1016/j.jenvman.2019.02.069

Premarathna, K. S. D., Rajapaksha, A. U., Sarkar, B., Kwon, E. E., Bhatnagar, A., Ok, Y. S., et al. (2019b). Biochar-based engineered composites for sorptive decontamination of water: A review. *Chem. Eng. J.* 372, 536–550. doi:10.1016/j.cej.2019.04.097

Puga, A. P., Abreu, C. A., Melo, L. C. A., and Beesley, L. (2016). Biochar application to a contaminated soil reduces the availability and plant uptake of zinc, lead and cadmium. *J. Environ. Manage.* 159, 86–93. doi:10.1016/j.jenvman.2015.05.036

Pusch, R. (2015). *Bentonite cay: Environmental properties and applications*. Boca Raton, FL, USA: CRC Press.

Qi, X., Xiao, S., Chen, X., Ali, I., Gou, J., and Wang, D. (2022). Biochar-based microbial agent reduces U and Cd accumulation in vegetables and improves rhizosphere microecology. *J. Hazard. Mater* 436, 129147. doi:10.1016/j.jhazmat.2022.129147

Qin, Q., Wang, Q., Fu, D., and Ma, J. (2011). An efficient approach for Pb (II) and Cd (II) removal using manganese dioxide formed *in situ*. *Chem. Eng. J.* 172, 68–74. doi:10.1016/j.cej.2011.05.066

Qiu, M., Liu, L., Ling, Q., Cai, Y., Yu, S., Wang, S., et al. (2022). Biochar for the removal of contaminants from soil and water: A review. *Biochar* 4, 19. doi:10.1007/s42773-022-00146-1

Qiu, Y., Zheng, Z., Zhou, Z., and Sheng, G. D. (2009). Effectiveness and mechanisms of dye adsorption on a straw-based biochar. *Bioresour. Technol.* 100, 5348–5351. doi:10.1016/j.biortech.2009.05.054

Rafiq, M. K., Bachmann, R. T., Rafiq, M. T., Shang, Z., Joseph, S., and Long, R. (2016). Influence of pyrolysis temperature on physico-chemical properties of corn stover (*Zea mays L*) biochar and feasibility for carbon capture and energy balance. *PLoS One* 11, e0156894. doi:10.1371/journal.pone.0156894

Rahman, M. A., Lamb, D., Rahman, M. M., Bahar, M. M., Sanderson, P., Abbasi, S., et al. (2020). Removal of arsenate from contaminated waters by novel zirconium and zirconium-iron modified biochar. *J. Hazard. Mat.* 409, 124488. doi:10.1016/j.jhazmat.2020.124488

Rahman, M. A., Lamb, D., Rahman, M. M., Bahar, M. M., and Sanderson, P. (2022). Adsorption-desorption behavior of arsenate using single and binary iron-modified biochars: Thermodynamics and redox transformation. *ACS Omega* 7, 101–117. doi:10.1021/acsomega.1c04129

Rajapaksha, A. U., Chen, S. S., Tsang, D. C. W., Zhang, M., Vithanage, M., Mandal, S., et al. (2016). Engineered/designer biochar for contaminant removal/immobilization from soil and water: Potential and implication of biochar modification. *Chemosphere* 148, 276–291. doi:10.1016/j.chemosphere.2016.01.043

Rajapaksha, A. U., Vithanage, M., Ahmad, M., Seo, D. C., Cho, J. S., Lee, S. E., et al. (2015). Enhanced sulfamethazine removal by steam-activated invasive plant-derived biochar. *J. Hazard. Mat.* 290, 43–50. doi:10.1016/j.jhazmat.2015.02.046

Rajapaksha, A. U., Vithanage, M., Jayarathna, L., and Kumara, C. K. (2011). Natural red Earth as a low cost material for arsenic removal: Kinetics and the effect of competing ions. *Appl. Geochem.* 26, 648–654. doi:10.1016/j.apgeochem.2011.01.021

Rawal, A., Joseph, S. D., Hook, J. M., Chia, C. H., Munroe, P. R., Donne, S., et al. (2016). Mineral-biochar composites: Molecular structure and porosity. *Environ. Sci. Technol.* 50, 7706–7714. doi:10.1021/acs.est.6b00685

Rizwan, M., Ali, S., Qayyum, M. F., Ibrahim, M., Rehman, M. Z., Abbas, T., et al. (2016). Mechanisms of biochar-mediated alleviation of toxicity of trace elements in plants: A critical review. *Environ. Sci. Pollut. Res.* 23, 2230–2248. doi:10.1007/s11356-015-5697-7

Sakhiya, A. K., Anand, A., and Kaushal, P. (2020). Production, activation, and applications of biochar in recent times. *Biochar* 2, 253–285. doi:10.1007/s42773-020-00047-1

Sarkar, B., Mandal, S., Tsang, Y. F., Kumar, P., Kim, K. H., and Ok, Y. S. (2018). Designer carbon nanotubes for contaminant removal in water and wastewater: A critical review. *Sci. Total Environ.* 612, 561–581. doi:10.1016/j.scitotenv.2017.08.132

Shaheen, S. M., Mosa, A., El-Naggar, A., Hossain, M. F., Abdelrahman, H., Niazi, N. K., et al. (2022). Manganese oxide-modified biochar: Production, characterization and applications for the removal of pollutants from aqueous environments-a review. *Bioresour. Technol.* 346, 126581. doi:10.1016/j.biortech.2021.126581

Shaheen, S. M., Niazi, N. K., Hassan, N. E., Bibi, I., Wang, H., Tsang, D. C., et al. (2019). Wood-based biochar for the removal of potentially toxic elements in water and wastewater: A critical review. *Int. Mat. Rev.* 64, 216–247. doi:10.1080/09506608.2018.1473096

Shakoor, M. B., Ye, Z. L., and Chen, S. (2021). Engineered biochars for recovering phosphate and ammonium from wastewater: A review. *Sci. Total Environ.* 779, 146240. doi:10.1016/j.scitotenv.2021.146240

Shang, J., Zong, M., Yu, Y., Kong, X., Du, Q., and Liao, Q. (2017). Removal of chromium (VI) from water using nanoscale zerovalent iron particles supported on herb-residue biochar. *J. Environ. Manage.* 197, 331–337. doi:10.1016/j.jenvman.2017.03.085

Shang, M. R., Liu, Y. G., Liu, S. B., Zeng, G. M., Tan, X. F., Jiang, L. H., et al. (2016). A novel graphene oxide coated biochar composite: Synthesis, characterization and application for Cr (VI) removal. *RSC Adv.* 6, 85202–85212. doi:10.1039/c6ra07151a

Shen, Z., Zhang, Y., McMillan, O., Jin, F., and Al-Tabbaa, A. (2017). Characteristics and mechanisms of nickel adsorption on biochars produced from wheat straw pellets and rice husk. *Environ. Sci. Pollut. Res.* 24, 12809–12819. doi:10.1007/s11356-017-8847-2

Siddiq, O. M., Tawabini, B. S., Soupios, P., and Ntarlagiannis, D. (2022). Removal of arsenic from contaminated groundwater using biochar: A technical review. *Int. J. Environ. Sci. Technol.* 19, 651–664. doi:10.1007/s13762-020-03116-x

Solanki, A., and Boyer, T. H. (2017). Pharmaceutical removal in synthetic human urine using biochar. *Environ. Sci. Water Res. Technol.* 3, 553–565. doi:10.1039/c6ew00224b

Spokas, K. A. (2010). Review of the stability of biochar in soils: Predictability of O:C molar ratios. *Carbon Manag.* 1, 289–303. doi:10.4155/cmt.10.32

Srivastav, A. L., Pham, T. D., Izah, S. C., Singh, N., and Singh, P. K. (2021). Biochar adsorbents for arsenic removal from water environment: A review. *Bull. Environ. Contam. Toxicol.* 108, 616–628. doi:10.1007/s00128-021-03374-6

Sun, H., Yang, J., Wang, Y., Liu, Y., Cai, C., and Davarpanah, A. (2021). Study on the removal efficiency and mechanism of tetracycline in water using biochar and magnetic biochar. *Coatings* 11, 1354. doi:10.3390/coatings11111354

Sun, K., Kang, M., Zhang, Z., Jin, J., Wang, Z., Pan, Z., et al. (2013). Impact of deashing treatment on biochar structural properties and potential sorption mechanisms of phenanthrene. *Environ. Sci. Technol.* 47, 11473–11481. doi:10.1021/es4026744

Sun, K., Ro, K., Guo, M., Novak, J., Mashayekhi, H., and Xing, B. (2011). Sorption of bisphenol A, 17α-Ethinyl estradiol and phenanthrene on thermally and hydrothermally produced biochars. *Bioresour. Technol.* 102, 5757–5763. doi:10.1016/j.biortech.2011.03.038

Sun, Y., Gao, B., Yao, Y., Fang, J., Zhang, M., Zhou, Y., et al. (2014). Effects of feedstock type, production method, and pyrolysis temperature on biochar and hydrochar properties. *Chem. Eng. J.* 240, 574–578. doi:10.1016/j.cej.2013.10.081

Sun, Y., Zheng, L., Zheng, X., Xiao, D., Yang, Y., Zhang, Z., et al. (2022). Adsorption of sulfonamides in aqueous solution on reusable coconut-shell biochar modified by alkaline activation and magnetization. *Front. Chem.* 9, 814647. doi:10.3389/fchem.2021.814647

Tag, A. T., Duman, G., Ucar, S., and Yanik, J. (2016). Effects of feedstock type and pyrolysis temperature on potential applications of biochar. *J. Anal. Appl. Pyrolysis* 120, 200–206. doi:10.1016/j.jaap.2016.05.006

Tan, X., Liu, S., Liu, Y., Gu, Y., Zeng, G., Cai, X., et al. (2016a). One-pot synthesis of carbon supported calcined-Mg/Al layered double hydroxides for antibiotic removal by slow pyrolysis of biomass waste. *Sci. Rep.* 6, 39691. doi:10.1038/srep39691

Tan, X., Liu, Y., Gu, Y., Xu, Y., Zeng, G., Hu, X., et al. (2016b). Biochar-based nano-composites for the decontamination of wastewater: A review. *Bioresour. Technol.* 212, 318–333. doi:10.1016/j.biortech.2016.04.093

Tang, J., Lv, H., Gong, Y., and Huang, Y. (2015). Preparation and characterization of a novel graphene/biochar composite for aqueous phenanthrene and mercury removal. *Bioresour. Technol.* 196, 355–363. doi:10.1016/j.biortech.2015.07.047

Thines, K. R., Abdullah, E. C., Mubarak, N. M., and Ruthiraan, M. (2017). Synthesis of magnetic biochar from agricultural waste biomass to enhancing route for waste water and polymer application: A review. *Renew. Sustain. Energy Rev.* 67, 257–276. doi:10.1016/j.rser.2016.09.057

Tian, X., Xie, Q., Chai, G., and Li, G. (2022). Simultaneous adsorption of As(III) and Cd(II) by ferrihydrite-modified biochar in aqueous solution and their mutual effects. *Sci. Rep.* 12, 5918. doi:10.1038/s41598-022-09648-1

Tomczyk, A., Boguta, P., and Sokołowska, Z. (2019). Biochar efficiency in copper removal from Haplic soils. *Int. J. Environ. Sci. Technol.* 16, 4899–4912. doi:10.1007/s13762-019-02227-4

Tomczyk, A., Sokolowska, Z., and Boguta, P. (2020). Biochar physicochemical properties: Pyrolysis temperature and feedstock kind effects. *Rev. Environ. Sci. Biotechnol.* 19, 191–215. doi:10.1007/s11157-020-09523-3

Trakal, L., Veselska, V., Safarik, I., Vitkova, M., Cihalova, S., and Komarek, M. (2016). Lead and cadmium sorption mechanisms on magnetically modified biochars. *Bioresour. Technol.* 203, 318–324. doi:10.1016/j.biortech.2015.12.056

Tripathi, M., Sahu, J. N., and Ganesan, P. (2016). Effect of process parameters on production of biochar from biomass waste through pyrolysis: A review. *Renew. Sustain. Energy Rev.* 55, 467–481. doi:10.1016/j.rser.2015.10.122

Tsai, W. T., and Chen, H. R. (2013). Adsorption kinetics of herbicide paraquat in aqueous solution onto a low-cost adsorbent, swine-manure derived biochar. *Int. J. Environ. Sci. Technol.* 10, 1349–1356. doi:10.1007/s13762-012-0174-z

Van Vinh, N., Zafar, M., Behera, S. K., and Park, H. S. (2015). Arsenic (III) removal from aqueous solution by raw and zinc-loaded pine cone biochar: Equilibrium, kinetics, and thermodynamics studies. *Int. J. Environ. Sci. Technol.* 12, 1283–1294. doi:10.1007/s13762-014-0507-1

Vimonses, V., Lei, S., Jin, B., Chow, C. W. K., and Saint, C. (2009). Adsorption of Congo red by three Australian kaolins. *Appl. Clay Sci.* 43, 465–472. doi:10.1016/j.clay.2008.11.008

Vitela-Rodriguez, A. V., and Rangel-Mendez, J. R. (2013). Arsenic removal by modified activated carbons with iron hydro (oxide) nanoparticles. *J. Environ. Manage.* 114, 225–231. doi:10.1016/j.jenvman.2012.10.004

Wainaina, S., Awasthi, M. K., Sarsaiya, S., Chen, H., Singh, E., Kumar, A., et al. (2020). Resource recovery and circular economy from organic solid waste using

aerobic and anaerobic digestion technologies. *Bioresour. Technol.* 301, 122778. doi:10.1016/j.biortech.2020.122778

Wan, S., Wang, S., Li, Y., and Gao, B. (2017). Functionalizing biochar with Mg–Al and Mg–Fe layered double hydroxides for removal of phosphate from aqueous solutions. *J. Ind. Eng. Chem.* 47, 246–253. doi:10.1016/j.jiec.2016.11.039

Wan, S., Wu, J., Zhou, S., Wang, R., Gao, B., and He, F. (2018). Enhanced lead and cadmium removal using biochar-supported hydrated manganese oxide (HMO) nanoparticles: Behavior and mechanism. *Sci. Total Environ.* 616-617, 1298–1306. doi:10.1016/j.scitotenv.2017.10.188

Wang, B., Gao, B., and Fang, J. (2017a). Recent advances in engineered biochar productions and applications. *Crit. Rev. Environ. Sci. Technol.* 47, 2158–2207. doi:10.1080/10643389.2017.1418580

Wang, B., Jiang, Y., Li, F., and Yang, D. (2017b). Preparation of biochar by simultaneous carbonization, magnetization and activation for norfloxacin removal in water. *Bioresour. Technol.* 233, 159–165. doi:10.1016/j.biortech.2017.02.103

Wang, H., Gao, B., Fang, J., Ok, Y. S., Xue, Y., Yang, K., et al. (2018). Engineered biochar derived from eggshell-treated biomass for removal of aqueous lead. *Ecol. Eng* 121, 124–129. doi:10.1016/j.ecoleng.2017.06.029

Wang, J., and Wang, S. (2019). Preparation, modification and environmental application of biochar: A review *J. Clean. Prod.* 227, 1002–1022.

Wang, J., Zhang, M., Zhou, R., Li, J., Zhao, W., and Zhou, J. (2020). Adsorption characteristics and mechanism of norfloxacin in water by γ-Fe_2O_3@BC. *Water Sci. Technol.* 82, 242–254. doi:10.2166/wst.2020.078

Wang, K., Peng, N., Lu, G., and Dang, Z. (2020). Effects of pyrolysis temperature and holding time on physicochemical properties of swine-manure-derived biochar. *Waste Biomass Valorization* 11, 613–624. doi:10.1007/s12649-018-0435-2

Wang, L., Ok, Y. S., Tsang, D. C. W., Alessi, D. S., Rinklebe, J., Masek, O., et al. (2021). Biochar composites: Emerging trends, field successes and sustainability implications. *Soil Use Manag.* 38, 14–38. doi:10.1111/sum.12731

Wang, L., Ok, Y. S., Tsang, D. C. W., Alessi, D. S., Rinklebe, J., Wang, H., et al. (2020). New trends in biochar pyrolysis and modification strategies: Feedstock, pyrolysis conditions, sustainability concerns and implications for soil amendment. *Soil Use manage.* 36, 1–29. doi:10.1016/j.jclepro.2019.04.282

Wang, M. C., Sheng, G. D., and Qiu, Y. P. (2015). A novel manganese-oxide/biochar composite for efficient removal of lead(II) from aqueous solutions. *Int. J. Environ. Sci. Technol.* 12, 1719–1726. doi:10.1007/s13762-014-0538-7

Wang, S., Gao, B., Zimmerman, A. R., Li, Y., Ma, L., Harris, W. G., et al. (2015). Removal of arsenic by magnetic biochar prepared from pinewood and natural hematite. *Bioresour. Technol.* 175, 391–395. doi:10.1016/j.biortech.2014.10.104

Wang, W., Wang, X., Wang, X., Yang, L., Wu, Z., Xia, S., et al. (2013). Cr (VI) removal from aqueous solution with bamboo charcoal chemically modified by iron and cobalt with the assistance of microwave. *J. Environ. Sci.* 25, 1726–1735. doi:10.1016/s1001-0742(12)60247-2

Wu, Q., Zou, D., Zheng, X., Liu, F., Li, L., and Xiao, Z. (2022). Effects of antibiotics on anaerobic digestion of sewage sludge: Performance of anaerobic digestion and structure of the microbial community. *Sci. Total Environ.* 845, 157384. doi:10.1016/j.scitotenv.2022.157384

Xiang, W., Zhang, X., Chen, J., Zou, W., He, F., Hu, X., et al. (2020). Biochar technology in wastewater treatment: A critical review. *Chemosphere* 252, 126539. doi:10.1016/j.chemosphere.2020.126539

Xiao, X., Chen, B., Chen, Z., Zhu, L., and Schnoor, J. L. (2018). Insight into multiple and multilevel structures of biochars and their potential environmental applications: A critical review. *Environ. Sci. Technol.* 52, 5027–5047. doi:10.1021/acs.est.7b06487

Xu, K., Lin, F., Dou, X., Zheng, M., Tan, W., and Wang, C. (2018). Recovery of ammonium and phosphate from urine as value-added fertilizer using wood waste biochar loaded with magnesium oxides. *J. Clean. Prod.* 187, 205–214. doi:10.1016/j.jclepro.2018.03.206

Xu, Q., Zhou, Q., Pan, M., and Dai, L. (2019). Interaction between chlortetracycline and calcium-rich biochar: Enhanced removal by adsorption coupled with flocculation. *Chem. Eng. J.* 382, 122705. doi:10.1016/j.cej.2019.122705

Xu, R. K., Xiao, S. C., Yuan, J. H., and Zhao, A. Z. (2011). Adsorption of methyl violet from aqueous solutions by the biochars derived from crop residues. *Bioresour. Technol.* 102, 10293–10298. doi:10.1016/j.biortech.2011.08.089

Xu, Y., Xie, X., Feng, Y., Ashraf, M. A., Liu, Y., Su, C., et al. (2020). As(III) and as(V) removal mechanisms by Fe-modified biochar characterized using synchrotron-based X-ray absorption spectroscopy and confocal micro-X-ray fluorescence imaging. *Bioresour. Technol.* 304, 122978. doi:10.1016/j.biortech.2020.122978

Xue, L., Gao, B., Wan, Y., Fang, J., Wang, S., Li, Y., et al. (2016). High efficiency and selectivity of MgFe-LDH modified wheat-straw biochar in the removal of nitrate from aqueous solutions. *J. Taiwan Inst. Chem. Eng.* 63, 312–317. doi:10.1016/j.jtice.2016.03.021

Yadav, A., Bagotia, N., Sharma, A. K., and Kumar, S. (2021). Advances in decontamination of wastewater using biomass-based composites: A critical review. *Sci. Total Environ.* 784, 147108. doi:10.1016/j.scitotenv.2021.147108

Yan, Y., Zhang, L., Feng, L., Sun, D., and Dang, Y. (2018). Comparison of varying operating parameters on heavy metals ecological risk during anaerobic co-digestion of chicken manure and corn stover. *Bioresour. Technol.* 247, 660–668. doi:10.1016/j.biortech.2017.09.146

Yang, G., Wu, L., Xian, Q., Shen, F., Wu, J., and Zhang, Y. (2016). Removal of Congo red and methylene blue from aqueous solutions by vermicompost-derived biochars. *PLoS One* 11, e0154562. doi:10.1371/journal.pone.0154562

Yang, X., Xu, G., Yu, H., and Zhang, Z. (2016). Preparation of ferric-activated sludge-based adsorbent from biological sludge for tetracycline removal. *Bioresour. Technol.* 211, 566–573. doi:10.1016/j.biortech.2016.03.140

Yang, X., Zhang, X., Wang, Z., Li, S., Zhao, J., Liang, G., et al. (2019). Mechanistic insights into removal of norfloxacin from water using different natural iron ore - biochar composites: More rich free radicals derived from natural pyrite-biochar composites than hematite-biochar composites. *Appl. Catal. B Environ.* 255, 117752. doi:10.1016/j.apcatb.2019.117752

Yao, Y., Gao, B., Chen, J., and Yang, L. (2013). Engineered biochar reclaiming phosphate from aqueous solutions: Mechanisms and potential application as a slow-release fertilizer. *Environ. Sci. Technol.* 47, 8700–8708. doi:10.1021/es4012977

Yao, Y., Gao, B., Fang, J., Zhang, M., Chen, H., Zhou, Y., et al. (2014). Characterization and environmental applications of clay–biochar composites. *Chem. Eng. J.* 242, 136–143. doi:10.1016/j.cej.2013.12.062

Yargicoglu, E. N., Sadasivam, B. Y., Reddy, K. R., and Spokas, K. (2015). Physical and chemical characterization of waste wood derived biochars. *Waste Manag.* 36, 256–268. doi:10.1016/j.wasman.2014.10.029

Yin, G., Tao, L., Chen, X., Bolan, N. S., Sarkar, B., Lin, Q., et al. (2021). Quantitative analysis on the mechanism of Cd^{2+} removal by $MgCl_2$-modified biochar in aqueous solutions. *J. Hazard. Mat.* 420, 126487. doi:10.1016/j.jhazmat.2021.126487

Zama, E. F., Zhu, Y. G., Reid, B. J., and Sun, G. X. (2017). The role of biochar properties in influencing the sorption and desorption of Pb (II), Cd (II) and as (III) in aqueous solution. *J. Clean. Prod.* 148, 127–136. doi:10.1016/j.jclepro.2017.01.125

Zhang, H., Chen, C., Gray, E. M., and Boyd, S. E. (2017). Effect of feedstock and pyrolysis temperature on properties of biochar governing end use efficacy. *Biomass Bioenergy* 105, 136–146. doi:10.1016/j.biombioe.2017.06.024

Zhang, J., Lu, M., Wan, J., Sun, Y., Lan, H., and Deng, X. (2018). Effects of pH, dissolved humic acid and Cu^{2+} on the adsorption of norfloxacin on montmorillonite-biochar composite derived from wheat straw. *Biochem. Eng. J.* 130, 104–112. doi:10.1016/j.bej.2017.11.018

Zhang, L., Lin, X., Wang, J., Jiang, F., Wei, L., Chen, G., et al. (2016). Effects of lead and mercury on sulfate-reducing bacterial activity in a biological process for flue gas desulfurization wastewater treatment. *Sci. Rep.* 6, 30455. doi:10.1038/srep30455

Zhang, M., Gao, B., Fang, J., Creamer, A. E., and Ullman, J. L. (2014). Self-assembly of needle-like layered double hydroxide (LDH) nanocrystals on hydrochar: Characterization and phosphate removal ability. *RSC Adv.* 4, 28171. doi:10.1039/c4ra02332c

Zhang, M., and Gao, B. (2013). Removal of arsenic, methylene blue, and phosphate by biochar/AlOOH nanocomposite. *Chem. Eng. J.* 226, 286–292. doi:10.1016/j.cej.2013.04.077

Zhang, M., Gao, B., Yao, Y., Xue, Y., and Inyang, M. (2012). Synthesis of porous MgO-biochar nanocomposites for removal of phosphate and nitrate from aqueous solutions. *Chem. Eng. J.* 210, 26–32. doi:10.1016/j.cej.2012.08.052

Zhang, X. N., Mao, G. Y., Jiao, Y. B., Shang, Y., and Han, R. P. (2014). Adsorption of anionic dye on magnesium hydroxide-coated pyrolytic bio-char and reuse by microwave irradiation. *Int. J. Environ. Sci. Technol.* 11, 1439–1448. doi:10.1007/s13762-013-0338-5

Zhang, X., Wang, H., He, L., Lu, K., Sarmah, J., Bolan, N. S., et al. (2013). Using biochar for remediation of soils contaminated with heavy metals and organic pollutants. *Environ. Sci. Pollut. Res.* 20, 8472–8483. doi:10.1007/s11356-013-1659-0

Zhang, Z., Zhu, Z., Shen, B., and Liu, L. (2019). Insights into biochar and hydrochar production and applications: A review. *Energy* 171, 581–598. doi:10.1016/j.energy.2019.01.035

Zhao, L., Cao, X., Masek, O., and Zimmerman, A. (2013). Heterogeneity of biochar properties as a function of feedstock sources and production temperatures. *J. Hazard. Mater* 256-257, 1–9. doi:10.1016/j.jhazmat.2013.04.015

Zhao, B., O'Connor, D., Zhang, J., Peng, T., Shen, Z., Tsang, D. C. W., et al. (2018). Effect of pyrolysis temperature, heating rate, and residence time on rapeseed stem derived biochar. *J. Clean. Prod.* 174, 977–987. doi:10.1016/j.jclepro.2017.11.013

Zhao, H., and Lang, Y. (2018). Adsorption behaviors and mechanisms of florfenicol by magnetic functionalized biochar and reed biochar. *J. Taiwan Inst. Chem. Eng.* 88, 152–160. doi:10.1016/j.jtice.2018.03.049

Zhao, S. X., Na, T., and Wang, X. D. (2017). Effect of temperature on the structural and physicochemical properties of biochar with apple tree branches as feedstock material. *Energies* 10, 1293. doi:10.3390/en10091293

Zheng, C., Yang, Z., Si, M., Zhu, F., Yang, W., Zhao, F., et al. (2020). Application of biochars in the remediation of chromium contamination: Fabrication, mechanisms, and interfering species. *J. Hazard. Mat.* 407, 124376. doi:10.1016/j.jhazmat.2020.124376

Zheng, J. L., Wang, S. J., Wang, R. M., Chen, Y. L., Siddique, K. H. M., Xia, G. M., et al. (2021). Ameliorative roles of biochar-based fertilizer on morpho-physiological traits, nutrient uptake and yield in peanut (*Arachis hypogaea L.*) under water stress. *Agric. Water Manag.* 257, 107129. doi:10.1016/j.agwat.2021.107129

Zheng, H., Wang, Z., Zhao, J., Herbert, S., and Xing, B. (2013). Sorption of antibiotic sulfamethoxazole varies with biochars produced at different temperatures. *Environ. Pollut.* 181, 60–67. doi:10.1016/j.envpol.2013.05.056

Zheng, X., Zou, D., Wu, Q., Wang, H., Li, S., Liu, F., et al. (2022). Review on fate and bioavailability of heavy metals during anaerobic digestion and composting of animal manure. *Waste Manag.* 150, 75–89. doi:10.1016/j.wasman.2022.06.033

Zheng, Y., Wang, B., Wester, A. E., Chen, J., He, F., Chen, H., et al. (2019). Reclaiming phosphorus from secondary treated municipal wastewater with engineered biochar. *Chem. Eng. J.* 362, 460–468. doi:10.1016/j.cej.2019.01.036

Zhou, Y., Gao, B., Zimmerman, A. R., Chen, H., Zhang, M., and Cao, X. (2014). Biochar-supported zerovalent iron for removal of various contaminants from aqueous solutions. *Bioresour. Technol.* 152, 538–542. doi:10.1016/j.biortech.2013.11.021

Zhou, Y., Gao, B., Zimmerman, A. R., Fang, J., Sun, Y., and Cao, X. (2013). Sorption of heavy metals on chitosan-modified biochars and its biological effects. *Chem. Eng. J.* 231, 512–518. doi:10.1016/j.cej.2013.07.036

Zhou, Y., Liu, X., Xiang, Y., Wang, P., Zhang, J., Zhang, F., et al. (2017). Modification of biochar derived from sawdust and its application in removal of tetracycline and copper from aqueous solution: Adsorption mechanism and modelling. *Bioresour. Technol.* 245, 266–273. doi:10.1016/j.biortech.2017.08.178

Zhu, D., and Pignatello, J. J. (2005). Characterization of aromatic compound sorptive interactions with black carbon (charcoal) assisted by graphite as a model. *Environ. Sci. Technol* 39, 2033–2041. doi:10.1021/es0491376

Zhu, N. M., Qiang, L., Guo, X. J., Zhang, H., and Deng, Y. (2014). Sequential extraction of anaerobic digestate sludge for the determination of partitioning of heavy metals. *Ecotoxicol. Environ. Saf.* 102, 18–24. doi:10.1016/j.ecoenv.2013.12.033

Zielinska, A., Oleszczuk, P., Charmas, B., Skubiszewska-Zieba, J., and Pasieczna-Patkowska, S. (2015). Effect of sewage sludge properties on the biochar characteristic. *J. Anal. Appl. Pyrol.* 112, 201–213. doi:10.1016/j.jaap.2015.01.025